

**Thermal Stabilization of Energetic Materials by the Aromatic Nitrogen-Rich
4,4',5,5'-Tetraamino-3,3'-Bi-1,2,4-Triazolium Cation**

Thomas M. Klapötke*, Philipp. C. Schmid, Simon Schnell and Jörg Stierstorfer^a

*Energetic Materials Research, Department of Chemistry,
University of Munich (LMU), Butenandtstr. 5-13, D-81377, Germany*
Fax: +49 89 2180 77492
E-mail: tmk@cup.uni-muenchen.de

Table of contents

1.	Materials and Methods.....	3
1.1.	NMR spectroscopy.....	3
1.2.	Vibrational spectroscopy	3
1.3.	Mass spectrometry and elemental analysis.....	3
1.4.	Differential thermal analysis	3
1.5.	Sensitivity testing	4
2.	Experimental work.....	4
2.1.	4,4',5,5'-Tetraamino-3,3'-bi-1,2,4-triazole (1)	4
2.2.	4,4',5,5'-Tetraamino-3,3'-bi-1,2,4-triazolium dinitramide (2)	5
2.3.	4,4',5,5'-Tetraamino-3,3'-bi-1,2,4-triazolium nitrotetrazolate-2-oxide (3).....	5
2.4.	4,4',5,5'-Tetraamino-3,3'-bi-1,2,4-triazolium nitrotetrazolate dihydrate (4)	6
2.5.	4,4',5,5'-Tetraamino-3,3'-bi-1,2,4-triazolium dinitrate (5)	7
2.6.	4,4',5,5'-Tetraamino-3,3'-bi-1,2,4-triazolium tetranitrobisimidazolate (6).....	7
2.7.	4,4',5,5'-Tetraamino-3,3'-bi-1,2,4-triazolium 5,5'-bitetrazole-1,1'-dioxide (7)	8
2.8.	4,4',5,5'-Tetraamino-3,3'-bi-1,2,4-triazolium 1,1'-dinitramino-5,5'-bitetrazolate (8).....	8
2.9.	4,4',5,5'-Tetraamino-3,3'-bi-1,2,4-triazolium nitriminotetrazolate hemihydrate (9) ..	9
2.10.	4,4',5,5'-Tetraamino-3,3'-bi-1,2,4-triazolium 1-methyl-5-nitriminotetrazolate dihydrate (10).....	9
2.11.	4,4',5,5'-Tetraamino-3,3'-bi-1,2,4-triazolium diperchlorate (11).....	10
2.12.	4,4',5,5'-Tetraamino-3,3'-bi-1,2,4-triazolium dipicrate (12).....	11
2.13.	4,4',5,5'-Tetraamino-3,3'-bi-1,2,4-triazolium dinitroformate (13).....	11
3.	X-ray Diffraction	13

3.1. Instrument and refinement software.....	13
3.2. Crystallographic data and refinement parameters	14
3.3. Crystal structures of compounds 4, 7 · 2 H ₂ O, 9–10 and 13	18
3.3.1. 4,4',5,5'-Tetraamino-3,3'-bi-1,2,4-triazolium nitrotetrazolate dihydrate (4)....	18
3.3.2. 4,4',5,5'-Tetraamino-3,3'-bi-1,2,4-triazolium bistetrazolate-1-oxide dihydrate (7 · 2 H ₂ O)	18
3.3.3. 4,4',5,5'-Tetraamino-3,3'-bi-1,2,4-triazolium 5-nitrimino-1 <i>H</i> -tetrazolate hemihydrate (9).....	20
3.3.4. 4,4',5,5'-Tetraamino-3,3'-bi-1,2,4-triazolium 1-methyl-5-nitriminetetrazolate dihydrate (10).....	23
3.3.5. 4,4',5,5'-Tetraamino-3,3'-bi-1,2,4-triazolium dinitroformate (13)	24
4. Electron Microscopy	25
5. Explosive performance	28
5.1. Heat of formation calculations	28
5.2. Energetic Performance	30
5.3. Small scale shock reactivity test.....	31
6. Toxicity assessment	32
7. Spectroscopy	33
7.1. NMR Spectroscopy	33
7.2. IR and Raman Spectroscopy	33
8. References.....	34

1. Materials and Methods

Caution! 4,4',5,5'-Tetraamino-3,3'-bi-1,2,4-triazole and its salts are energetic materials with sensitivities towards shock and friction. Therefore, proper security precautions (safety glass, face shield, earthened equipment and shoes, Kevlar gloves and ear plugs) have to be applied while synthesizing and handling the described compounds. Specifically, compounds described having the azido group are extremely sensitive and have to be handled very carefully.

All chemicals and solvents were employed as received (Sigma-Aldrich, Fluka, Acros) without further purification unless otherwise stated.

1.1. NMR spectroscopy

^1H and ^{13}C NMR spectra were recorded using a JEOL Eclipse 270, JEOL EX 400 or a JEOL Eclipse 400 instrument. The chemical shifts quoted in ppm in the text refer to tetramethylsilane (^1H , ^{13}C).

1.2. Vibrational spectroscopy

Infrared spectra were measured using a Perkin Elmer Spectrum One FT-IR spectrometer as KBr pellets. Raman spectra were recorded on a Bruker MultiRAM Raman Sample Compartment D418 equipped with a Nd-YAG-Laser (1064 nm) and a LN-Ge diode as detector.

1.3. Mass spectrometry and elemental analysis

Mass spectra of the described compounds were measured at a JEOL MStation JMS 700 using either DEI or FAB technique. To measure elemental analyses a Netsch STA 429 simultaneous thermal analyzer was employed.

1.4. Differential thermal analysis

Differential thermal analysis (DTA) measurements to determine the decomposition temperatures of compound **1–13** were performed at a heating rate of 5°C min^{-1} with an OZM Research DTA 552-Ex instrument.

1.5. Sensitivity testing

The impact sensitivity tests were carried out according to STANAG 4489¹ modified instruction² using a BAM (Bundesanstalt für Materialforschung) drop hammer.³ The friction sensitivity tests were carried out according to STANAG 4487⁴ modified instruction⁵ using the BAM friction tester. The classification of the tested compounds results from the “UN Recommendations on the Transport of Dangerous Goods”.⁶ Additionally all compounds were tested upon the sensitivity towards electrical discharge using the Electric Spark Tester ESD 2010 EN.⁷

2. Experimental work

2.1. 4,4',5,5'-Tetraamino-3,3'-bi-1,2,4-triazole (1)

4,4',5,5'-Tetraamino-3,3'-bi-1,2,4-triazole (**1**) was synthesized according to the literature:⁸ Phosphorus pentoxide (10 g, 70.4 mmol) was slowly dissolved in phosphoric acid (30 g, 306 mmol), which was preheated to 50 °C. A finely grinded mixture of oxalic acid dihydrate (3.15 g, 25.0 mmol, 1.0 eq) and diaminoguanidine monohydrochloride (8.29 g, 66 mmol, 2.6 eq.) was slowly added to the preheated solution. After complete addition, the viscous mixture was slowly heated to 120 °C and gas evolution of HCl was observed. The mixture was kept at 120 °C for 4 h and was then cooled to room temperature under stirring. 150 mL ice water was poured into the mixture and a white precipitate was formed. About 75 mL of 10 M NaOH was used to neutralize the reaction mixture, changing the color of the suspension from white to brown. The precipitate was filtered, washed repeatedly with water and air dried to obtain crude compound **1** as a brownish solid. Yield: 1.39 g, 7.09 mmol, 28%.

For purification the crude product was recrystallized with hydrochloric acid or glacial acetic acid. Compound **1** (1000 mg, 5.10 mmol, 1.00 eq.) was added slowly to glacial acid. The mixture was heated until compound **1** completely dissolved. The mixture was removed from the heating bath and was left to cool to room temperature. After filtration and repeated washing with water the residue was dried in a nitrogen flow before drying the substance in oven at 100 °C over night. Then the solid was suspended in 50 mL water and basified with about 1 mL of 10 M NaOH. The suspension was filtered and the residue was air dried to obtain pure compound **1** as a white solid. Yield: 696 mg, 3.55 mmol, 70%.

DTA (5 °C min⁻¹) onset: 342 °C (dec.); IR (ATR, cm⁻¹): $\tilde{\nu}$ = 3782(vw), 3400(m), 3341(m), 3278(m), 3142(w), 2348(vw), 1626(vs), 1537(s), 1478(m), 1421(w), 1317(w), 1252(vw),

1232(vw), 1085(m), 1022(m), 987(vs), 935(m), 799(vw), 778(vw), 723(m), 678(vw), 664(vw); Raman (1064 nm, 300 mW, 25 °C, cm⁻¹): $\tilde{\nu}$ = 3258(4), 3171(3), 1592(100), 1551(11), 1510(4), 1393(4), 1289(7), 1087(10), 1034(6), 811(16), 712(6), 621(3), 374(3), 330(4), 268(4), 110(12), 93(7); ¹H NMR ([D₆]DMSO): δ = 5.91 (br s, 4H), 5.81 ppm (br s, 4H); ¹³C NMR ([D₆]DMSO): δ = 155.4 (s, C–NH₂), 139.4 ppm (s, C–C); *m/z* (DEI⁺): 196.2 (C₄H₈N₁₀); EA (C₄H₈N₁₀, 196.17): C 24.49, H 4.11, N 71.40; found: C 25.04, H 4.04, N 69.93; BAM impact: 40 J, BAM friction: 360 N, ESD: 1.5 J (at grain sizes: <100 μm).

2.2. 4,4',5,5'-Tetraamino-3,3'-bi-1,2,4-triazolium dinitramide (2)

To a suspension of 4,4',5,5'-tetraamino-3,3'-bi-1,2,4-triazole (**1**) (392 mg, 2.00 mmol, 1.00 eq.) and ammonium dinitramide (496 mg, 4.00 mmol, 2.00 eq.) in water was added 1 mL 1 M hydrochloric acid. The mixture was heated until all components were dissolved and the mixture was left to crystallize over night. The product was obtained in form of slightly brownish crystals. Yield: 416 mg, 1.01 mmol, 51%.

DTA (5 °C min⁻¹) onset: 200 °C (dec.); IR (ATR, cm⁻¹): $\tilde{\nu}$ = 3278(m), 3142(m), 3088(m), 2854(m), 1695(vs), 1602(m), 1596(m), 1554(m), 1516(s), 1470(m), 1417(m), 1352(m), 1339(m), 1306(m), 1258(m), 1172(s), 1082(w), 992(vs), 954(m), 790(m), 778(m), 706(w), 672(w), 672(w); Raman (1064 nm, 300 mW, 25 °C, cm⁻¹): $\tilde{\nu}$ = 3176(1), 1695(2), 1642(100), 1560(2), 1532(1), 1436(6), 1377(1), 1339(2), 1288(14), 1124(2), 1079(7), 1022(2), 805(20), 713(7), 602(6), 492(1), 415(1), 387(2), 328(3), 286(2), 264(2), 175(3), 150(7), 150(7), 121(12), 90(11); ¹H NMR ([D₆]DMSO): δ = 8.56 (br s, 4 H), 6.08 ppm (br s, 6 H); ¹³C NMR ([D₆]DMSO): δ = 152.0 (s, C–NH₂), 137.8 ppm (s, C–C); *m/z* (FAB⁻): 106.0 (N₃O₄⁻), *m/z* (FAB⁺): 197.0 (C₄H₉N₁₀⁺); EA (C₄H₁₀N₁₆O₈, 410.22): C 11.71, H 2.46, N 54.63; found: C 12.04, H 2.55, N 53.96; BAM impact: 5 J, BAM friction: 360 N, ESD: 0.8 J (at grain sizes <100 μm).

2.3. 4,4',5,5'-Tetraamino-3,3'-bi-1,2,4-triazolium nitrotetrazolate-2-oxide (3)

To 4,4',5,5'-tetraamino-3,3'-bi-1,2,4-triazole (**1**) (392 mg, 2.00 mmol, 1.00 eq.) and ammonium nitrotetrazolate-2-oxide (592 mg, 4.00 mmol, 2.00 eq.) in water 1 mL 2 M hydrochloric acid was added and the suspension was heated until all components dissolved. The reaction mixture was cooled to room temperature and was then left to crystallize over night, yielding yellow crystals. Yield: 631 mg, 1.38 mmol, 69%.

DTA ($5\text{ }^{\circ}\text{C min}^{-1}$) onset: $220\text{ }^{\circ}\text{C}$ (dec.); IR (ATR, cm^{-1}): $\tilde{\nu} = 3432(\text{m}), 3379(\text{s}), 3294(\text{m}), 3106(\text{s}), 2673(\text{m}), 1757(\text{w}), 1704(\text{s}), 1613(\text{s}), 1540(\text{vs}), 1532(\text{vs}), 1467(\text{m}), 1456(\text{m}), 1426(\text{s}), 1403(\text{vs}), 1381(\text{s}), 1305(\text{vs}), 1257(\text{s}), 1232(\text{vs}), 1091(\text{m}), 1075(\text{s}), 1049(\text{s}), 975(\text{s}), 904(\text{s}), 904(\text{s}), 822(\text{m}), 761(\text{m}), 707(\text{m}), 701(\text{s}), 664(\text{s})$; Raman ($1064\text{ nm}, 300\text{ mW}, 25\text{ }^{\circ}\text{C}, \text{cm}^{-1}$): $\tilde{\nu} = 3299(2), 1715(2), 1637(42), 1592(3), 1535(5), 1460(6), 1424(29), 1401(63), 1385(20), 1308(14), 1292(10), 1234(7), 1122(4), 1091(9), 1073(49), 1052(28), 982(100), 843(3), 804(20), 761(4), 720(4), 705(4), 610(4), 610(4), 604(5), 489(3), 338(5), 275(3), 240(5), 206(7), 179(4), 144(11), 125(24), 104(21), 72(17)$; $^1\text{H NMR}$ ($[\text{D}_6]\text{DMSO}$): $\delta = 8.64$ (br s, 4 H), 6.14 ppm (br s, 6 H); $^{13}\text{C NMR}$ ($[\text{D}_6]\text{DMSO}$): $\delta = 157.4$ (s, C–NO₂), 152.0 (s, C–NH₂), 137.9 ppm (s, C–C); m/z (FAB[−]): 130.0 (CN₅O₃[−]), m/z (FAB⁺): 197.0 (C₄H₉N₁₀⁺); EA (C₆H₁₀N₂₀O₆, 458.28): C 15.73, H 2.20, N 61.13; found: C 16.05, H 2.24, N 60.57; BAM impact: 6 J, BAM friction: 360 N, ESD: 0.8 J (at grain sizes 100 – 500 μm).

2.4. 4,4',5,5'-Tetraamino-3,3'-bi-1,2,4-triazolium nitrotetrazolate dihydrate (4)

To a suspension of 4,4',5,5'-tetraamino-3,3'-bi-1,2,4-triazole (**1**) (196 mg, 1.00 mmol, 1.00 eq.) and ammonium nitrotetrazolate (264 mg, 2.00 mmol, 2.00 eq.) in water 1 mL 2 M hydrochloric acid was added and the reaction mixture was heated until all solid materials were dissolved. After crystallization over night compound **4** was obtained in form of brownish crystals. Yield: 312 mg, 0.67 mmol, 67%.

DTA ($5\text{ }^{\circ}\text{C min}^{-1}$) onset: $89\text{ }^{\circ}\text{C}$ (−H₂O), $225\text{ }^{\circ}\text{C}$ (dec.); IR (ATR, cm^{-1}): $\tilde{\nu} = 3568(\text{m}), 3338(\text{m}), 3250(\text{m}), 3143(\text{m}), 2946(\text{w}), 2850(\text{w}), 2755(\text{m}), 1697(\text{vs}), 1611(\text{m}), 1584(\text{w}), 1538(\text{vs}), 1511(\text{w}), 1494(\text{w}), 1436(\text{m}), 1417(\text{s}), 1316(\text{s}), 1264(\text{w}), 1179(\text{w}), 1167(\text{w}), 1098(\text{w}), 1049(\text{w}), 1028(\text{w}), 984(\text{s}), 984(\text{s}), 937(\text{m}), 838(\text{s}), 785(\text{w}), 736(\text{vw}), 712(\text{w}), 671(\text{w})$; Raman ($1064\text{ nm}, 300\text{ mW}, 25\text{ }^{\circ}\text{C}, \text{cm}^{-1}$): $\tilde{\nu} = 3264(2), 1709(4), 1648(100), 1605(5), 1540(8), 1484(4), 1414(94), 1335(2), 1314(6), 1298(12), 1178(3), 1168(6), 1134(6), 1089(6), 1077(4), 1067(3), 1063(3), 1049(85), 1043(38), 1031(7), 944(2), 837(10), 802(22), 802(22), 774(5), 716(10), 692(4), 614(3), 538(5), 451(5), 422(3), 380(5), 330(10), 280(7), 260(10), 175(11), 123(30), 86(76), 64(22)$; $^1\text{H NMR}$ ($[\text{D}_6]\text{DMSO}$): $\delta = 8.64$ (br s, 4 H), 6.16 ppm (br s, 6 H); $^{13}\text{C NMR}$ ($[\text{D}_6]\text{DMSO}$): $\delta = 168.8$ (s, C–NO₂), 152.0 (s, C–NH₂), 137.8 ppm (s, C–C); m/z (FAB[−]): 114.0 (CN₅O₂[−]), m/z (FAB⁺): 197.0 (C₄H₉N₁₀⁺); EA (C₆H₁₄N₂₀O₆, 462.31): C 15.59, H 3.05, N 60.59; found: C 15.84, H 3.06, N 59.48; BAM impact: 35 J, BAM friction: 360 N, ESD: 0.30 J (at grain sizes <100 μm).

2.5. 4,4',5,5'-Tetraamino-3,3'-bi-1,2,4-triazolium dinitrate (5)

4,4',5,5'-Tetraamino-3,3'-bi-1,2,4-triazole) (**1**) (140 mg, 0.71 mmol 1.00 eq.) was added to 0.75 mL of a 2 M HNO₃ in 5 mL water. The suspension was heated to reflux and left standing overnight to yield colorless crystals. Yield: 0.20 g, 0.62 mmol, 87%.

DTA (5 °C min⁻¹) onset: 275 °C (dec.); IR (ATR, cm⁻¹): $\tilde{\nu}$ = 3329(s), 3253(m), 3201(m), 3115(m), 2913(m), 2620(m), 1756(vw), 1685(s), 1611(m), 1575(m), 1523(w), 1406(m), 1313(vs), 1294(s), 1249(s), 1148(m), 1095(w), 1047(m), 981(m), 942(m), 849(m), 820(m), 778(m), 778(m), 736(vw), 723(w), 685(m), 666(m); Raman (1064 nm, 300 mW, 25 °C, cm⁻¹): $\tilde{\nu}$ = 3235(3), 1703(5), 1656(6), 1639(100), 1588(7), 1539(3), 1461(6), 1384(3), 1289(13), 1128(6), 1085(9), 1067(4), 1051(39), 1034(3), 952(3), 800(21), 728(5), 712(10), 614(5), 576(3), 415(4), 383(4), 340(5), 340(5), 266(5), 172(14), 142(22), 128(24), 111(22), 69(6); ¹H NMR ([D₆]DMSO): δ = 8.57 (br s, 4 H), 6.14 ppm (br s, 6 H); ¹³C NMR ([D₆]DMSO): δ = 152.0 (s, C–NH₂), 137.8 ppm (s, C–C); *m/z* (FAB⁻): 62.0 (NO₃⁻), *m/z* (FAB⁺): 197.0 (C₄H₁₀N₁₂O₆, 322.20); EA (C₄H₁₀N₁₂O₆, 322.20): C 14.91, H 3.13, N 52.17; found: C 15.17, H 3.08, N 51.56; BAM impact: 15 J, BAM friction: 360 N, ESD: 1.5 J (at grain sizes 100 – 500 µm).

2.6. 4,4',5,5'-Tetraamino-3,3'-bi-1,2,4-triazolium tetranitrobisimidazolate (6)

4,4',5,5'-Tetraamino-3,3'-bi-1,2,4-triazole (**1**) (196 mg, 1.00 mmol, 1.00 eq.), ammonium tetranitrobisimidazolate (348 mg, 1 mmol, 1.00 eq.) and 2 mL 1 M hydrochloric acid were added to 1.5 L of water. The formed suspension was refluxed for 5 min and a yellowish solution was formed. The solution was left to cool to room temperature and cooled to 5 °C over night. Filtration of the solution yielded yellow crystals of compound **6**. Yield: 290.0 mg, 0.57 mmol, 57 %.

DTA (5 °C min⁻¹) onset: 290 °C (dec.); IR (ATR, cm⁻¹): $\tilde{\nu}$ = 3379(w), 2919(w), 1699(s), 1528(m), 1497(m), 1487(s), 1386(s), 1366(vs), 1300(s), 1237(s), 1215(s), 1114(m), 1062(m), 973(m), 899(m), 853(m), 809(vs), 751(m), 695(m), 675(w); Raman (1064 nm, 300 mW, 25 °C, cm⁻¹): $\tilde{\nu}$ = 1808(2), 1641(31), 1620(12), 1550(100), 1539(50), 1507(8), 1489(34), 1387(15), 1351(19), 1297(63), 1269(30), 1236(61), 1112(3), 1069(4), 1035(6), 1024(14), 874(19), 810(4), 803(4), 770(4), 760(5), 755(5), 704(3), 704(3), 617(2), 524(3), 394(5), 342(3), 263(5), 199(8), 118(12), 101(16); ¹H NMR ([D₆]DMSO): δ = 8.10 (br s, 4 H), 6.17 ppm (br s, 4 H); ¹³C NMR ([D₆]DMSO): δ = 152.8 (s, C–NH₂ Cation), 141.7 (s, C–C_{Anion}), 139.4 (s, C=C_{Anion}), 138.1 ppm (s, C–C_{Cation}); *m/z* (ESI⁻): 313.0 (C₆HO₈N₈⁻), *m/z* (ESI⁺): 197.1

(C₄H₉N₁₀⁺); EA (C₁₀H₁₀N₁₈O₈, 510.31): C 23.54, H 1.98, N 49.41; found: C 23.76, H 2.18, N 48.53; BAM impact 40 J, BAM friction: 360 N, ESD 0.4 J (at grain sizes 100 – 500 µm).

2.7. 4,4',5,5'-Tetraamino-3,3'-bi-1,2,4-triazolium 5,5'-bitetrazole-1,1'-dioxide (7)

A clear solution of 5,5'-di-1,1'-hydroxytetrazole dihydrate (206 mg, 1.00 mmol, 1.0 eq.) and 4,4',5,5'-tetraamino-3,3'-bi-1,2,4-triazole (**1**) (196 mg, 1.00 mmol, 1.00 eq.) was prepared by dissolving the components in water (150 mL) while heating. The reaction mixture was refluxed for 10 min. and was then left to crystallize over night, yielding compound **7** as colorless crystals. Yield: 340 mg, 0.92 mmol, 92%.

DTA (5 °C min⁻¹) onset: 279 °C (dec.); IR (ATR, cm⁻¹): $\tilde{\nu}$ = 3360(w), 2964(m), 2671(w), 1694(vs), 1596(w), 1529(w), 1468(w), 1400(m), 1348(m), 1302(w), 1282(w), 1263(vw), 1236(s), 1225(m), 1171(m), 1065(vw), 1041(w), 1001(m), 970(s), 924(m), 787(w), 773(w), 732(m), 732(m), 714(w), 669(w); Raman (1064 nm, 300 mW, 25 °C, cm⁻¹): $\tilde{\nu}$ = 3214(3), 1709(4), 1633(100), 1603(73), 1598(72), 1575(5), 1558(4), 1537(3), 1457(6), 1437(6), 1297(13), 1281(7), 1247(10), 1234(17), 1142(17), 1110(11), 1089(10), 1005(6), 808(25), 770(6), 740(2), 714(5), 607(5), 607(5), 418(5), 404(5), 384(4), 342(6), 290(5), 275(7), 264(4), 198(4), 134(30), 121(33), 102(12), 94(11), 67(12); ¹H NMR ([D₆]DMSO): δ = 7.65 (br s, 6 H), 6.00 ppm (br s, 4 H); ¹³C NMR ([D₆]DMSO): δ = 153.6 (s, C–NH₂ Cation), 138.5 (C–C_{Cation}), 135.2 (s, C–C_{Anion}); *m/z* (FAB⁻): 169.0 (C₂HN₈O₂⁻), *m/z* (FAB⁺): 197.0 (C₄H₉N₁₀⁺); EA (C₆H₁₀N₁₈O₂, 366.26): C 19.68, H 2.75, N 68.84; found: C 20.12, H 2.76, N 68.41; BAM impact: 40 J, BAM friction: 360 N, ESD: 1.5 J (at grain sizes <100 µm).

2.8. 4,4',5,5'-Tetraamino-3,3'-bi-1,2,4-triazolium 1,1'-dinitramino-5,5'-bitetrazolate (8)

4,4',5,5'-Tetraamino-3,3'-bi-1,2,4-triazole (**1**) (196 mg, 1.00 mmol, 1.00 eq.) and dihydroxylammonium 1,1'-dinitramino-5,5'-bitetrazolate (324 mg, 1.00 mmol, 1.00 eq.) were dissolved in water under heating and the solution was left to stand overnight yielding colorless crystals of compound **8**. Yield: 276 mg, 0.61 mmol, 61%.

DTA (5 °C min⁻¹) onset: 223 °C (dec.); IR (ATR, cm⁻¹): 3417(m), 3331(s), 3215(s), 3137(m), 2932(m), 2733(m), 2350(w), 2290(m), 1698(vs), 1616(s), 1530(m), 1485(w), 1416(s), 1361(s), 1285(vs), 1254(vs), 1162(m), 1119(m), 1035(w), 993(s), 962(m), 874(m), 770(s), 770(s), 710(s), 666(w); Raman (1064 nm, 300 mW, 25 °C, cm⁻¹): $\tilde{\nu}$ = 3237(1), 1705(3), 1648(100), 1611(66), 1585(6), 1540(3), 1448(9), 1433(4), 1295(13), 1264(18), 1254(15),

1141(7), 1082(15), 1023(24), 989(4), 894(3), 805(11), 722(5), 711(5), 608(4), 520(7), 456(3), 411(3), 411(3), 375(3), 321(8), 304(7), 279(5), 263(5), 175(4), 154(11), 134(29), 114(47), 94(35), 65(7); ^1H NMR ([D₆]DMSO): δ = 8.60 (br s, 4 H), 6.13 ppm (br s, 4 H); ^{13}C NMR ([D₆]DMSO): δ = 151.9 (s, C–NH₂ Cation), 140.5 (s, C–C Anion), 137.7 ppm (s, C–C Cation); *m/z* (FAB[−]): 255.0 (C₂HN₁₂O₄[−]), *m/z* (FAB⁺): 197.0 (C₄H₉N₁₀⁺); EA (C₆H₁₀N₂₂O₄, 454.30): C 15.86, H 2.22, N 67.83; found: C 16.06, H 2.24, N 67.83; BAM impact: 3 J, BAM friction: 10 N, ESD: 50 mJ (at grain sizes 100 – 500 μm).

2.9. 4,4',5,5'-Tetraamino-3,3'-bi-1,2,4-triazolium nitriminotetrazolate hemihydrate (9)

To a suspension of 4,4',5,5'-tetraamino-3,3'-bi-1,2,4-triazole (**1**) (392 mg, 2.00 mmol, 1.00 eq.) and potassium nitriminotetrazolate (672 mg, 4.00 mmol, 2.00 eq.) in water 1 mL 2 M hydrochloric acid was added. The suspension was heated until all solid materials were dissolved, before the mixture was left to crystallize over night and compound **9** was obtained as brownish crystals. Yield: 243 mg, 0.71 mmol, 71 %.

DTA (5 °C min^{−1}) onset: 232 °C; IR (ATR, cm^{−1}): $\tilde{\nu}$ = 3491(m), 3447(s), 3356(s), 3320(s), 2926(m), 1703(s), 1644(s), 1607(s), 1552(m), 1520(m), 1486(m), 1445(s), 1391(w), 1321(vs), 1298(s), 1241(s), 1142(m), 1095(m), 1055(m), 1043(m), 1026(s), 975(m), 964(m), 964(m), 930(s), 873(m), 781(w), 772(w), 745(w), 721(w), 709(m), 698(w), 674(w), 656(vw); Raman (1064 nm, 300 mW, 25 °C, cm^{−1}): 3359(2), 1709(2), 1642(24), 1615(30), 1600(100), 1576(8), 1559(15), 1543(8), 1523(17), 1481(4), 1446(3), 1410(6), 1399(8), 1392(8), 1351(8), 1289(10), 1245(3), 1124(6), 1103(5), 1087(9), 1061(10), 1030(6), 1002(6), 1002(6), 886(4), 800(26), 755(4), 719(5), 617(4), 476(4), 426(4), 376(3), 325(3), 262(5), 246(5), 168(8), 119(20), 85(12), 73(21); ^1H NMR ([D₆]DMSO): δ = 7.82 (br s, 4 H), 6.05 ppm (br s, 6 H); ^{13}C NMR ([D₆]DMSO): δ = 157.7 (s, C=N–NO₂), 153.3 (s, C–NH₂), 138.4 ppm (s, C–C); *m/z* (FAB[−]): 129.0 (CHN₆O[−]), *m/z* (FAB⁺): 197.0 (C₄H₉N₁₀⁺); EA (C₁₀H₂₂N₃₂O₅, 670.51): C 17.91, H 3.31, N 66.85; found: C 17.34, H 3.81, N 62.00; BAM impact: 40 J, BAM friction: 360 N, ESD: 1.5 J (at grain sizes 500 – 1000 μm).

2.10. 4,4',5,5'-Tetraamino-3,3'-bi-1,2,4-triazolium 1-methyl-5-nitriminotetrazolate dihydrate (10)

4,4',5,5'-Tetraamino-3,3'-bi-1,2,4-triazole (**1**) (392 mg, 2.00 mmol, 1.00 eq.), ammonium 1-methylnitriminotetrazolate (644 mg, 4.00 mmol, 2.00 eq.) and 1 mL 2 M hydrochloric acid

were dissolved in water under heating and the solution was left to crystallize over night to give compound **10** as colorless needles. Yield: 804 mg, 1.66 mmol, 83%.

DTA (5 °C min⁻¹) onset: 104 °C (–H₂O), 209 °C (dec.); IR (ATR, cm⁻¹): $\tilde{\nu}$ = 3331(m), 1695(s), 1600(m), 1505(m), 1459(m), 1351(s), 1332(vs), 1296(s), 1241(m), 1110(m), 1049(w), 1028(m), 986(s), 959(m), 911(m), 877(m), 775(m), 750(w), 735(w), 691(m), 671(m); Raman (1064 nm, 300 mW, 25 °C, cm⁻¹): $\tilde{\nu}$ = 2965(3), 1695(3), 1649(100), 1496(34), 1457(16), 1408(4), 1342(7), 1303(15), 1142(6), 1109(8), 1050(5), 1030(41), 987(4), 879(5), 802(18), 751(4), 745(3), 714(8), 701(7), 491(7), 452(3), 368(4), 331(9), 331(9), 296(12), 262(5), 242(4), 204(7), 178(9), 113(27), 87(25), 70(14), 63(8); ¹H NMR ([D₆]DMSO): δ = 6.89 (br s, 4 H), 5.99 (br s, 6 H), 1.30 ppm (s, 3H, –CH₃); ¹³C NMR ([D₆]DMSO): δ = 155.4 (s, C=N–NO₂), 152.9 (s, C–NH₂), 138.2 ppm (s, C–C), 32.9 ppm (s, –CH₃); *m/z* (FAB[−]): 143.0 (C₂H₃N₆O₂[−]), *m/z* (FAB⁺): 197.0 (C₄H₉N₁₀⁺); EA (C₈H₂₀N₂₂O₆, 520.40): C 18.46, H 3.87, N 59.22; found: C 18.72, H 3.81, N 58.82; BAM impact: 35 J, BAM friction: 360 N, ESD: 0.5 J (at grain sizes 500 – 1000 µm).

2.11. 4,4',5,5'-Tetraamino-3,3'-bi-1,2,4-triazolium diperchlorate (11)

To 4,4',5,5'-tetraamino-3,3'-bi-1,2,4-triazole (**1**) (196 mg, 1.00 mmol, 1.00 eq.) in 50 mL water 4 mL 1 M perchloric acid was added and the solution was heated until all solid components were dissolved. The solution was left to crystallize over night to yield compound **11** as colorless needles. Yield: 317 mg, 0.80 mmol, 40%.

DTA (5 °C min⁻¹) onset: 286 °C (dec.); IR (ATR, cm⁻¹): $\tilde{\nu}$ = 3625(vw), 3557(vw), 3417(m), 3349(m), 3307(m), 3213(m), 1703(s), 1615(m), 1564(w), 1528(w), 1486(vw), 1375(vw), 1313(w), 1257(vw), 1099(vs), 1045(vs), 986(s), 956(m), 928(m), 782(w), 693(w), 673(w); Raman (1064 nm, 300 mW, 25 °C, cm⁻¹): $\tilde{\nu}$ = 3314(3), 1716(3), 1652(100), 1569(4), 1544(2), 1450(10), 1296(17), 1138(5), 1075(6), 929(37), 806(26), 719(11), 630(8), 604(4), 467(9), 459(8), 381(4), 334(4), 285(2), 260(2), 87(31); ¹H NMR ([D₆]DMSO): δ = 8.61 (br s, 4 H), 6.08 ppm (br s, 6 H); ¹³C NMR ([D₆]DMSO): δ = 152.0 (s, C–NH₂), 137.9 ppm (s, C–C); *m/z* (FAB[−]): 99.1 (ClO₄[−]), *m/z* (FAB⁺): 197.0 (C₄H₉N₁₀⁺); EA (C₄H₁₀Cl₂N₁₀O₈, 397.09): C 12.10, H 2.54, N 35.27, Cl 17.86; found: C 12.32, H 2.55, N 35.24 C 18.22; BAM impact: 5 J, BAM friction: 240 N, ESD: 0.6 J (at grain sizes 100 – 500 µm).

2.12. 4,4',5,5'-Tetraamino-3,3'-bi-1,2,4-triazolium dipicrate (12)

4,4',5,5'-Tetraamino-3,3'-bi-1,2,4-triazole (**1**) (196.2 mg, 1.00 mmol, 1.00 eq.) and picric acid (448.2 mg, 2.00 mmol, 2.00 eq.) were dissolved in water under heating so that a clear solution was observed. The solution was cooled down to room temperature and left standing over night to yield compound **12** in form of a yellowish solid. Yield: 484 mg, 0.74 mmol, 74%.

DTA (5 °C min⁻¹) onset: 284 °C (dec.); IR (ATR, cm⁻¹): $\tilde{\nu}$ = 3329(m), 3194(m), 3076(m), 1695(s), 1630(s), 1616(s), 1565(s), 1520(s), 1474(s), 1422(s), 1363(s), 1326(vs), 1265(vs), 1160(s), 1086(s), 1060(m), 978(m), 928(m), 916(s), 837(m), 790(s), 776(m), 744(m), 744(m), 714(s), 681(m); Raman (1064 nm, 300 mW, 25 °C, cm⁻¹): $\tilde{\nu}$ = 3074(2), 1640(32), 1545(28), 1497(12), 1435(5), 1368(33), 1340(48), 1315(100), 1273(30), 1165(17), 1118(5), 1089(10), 1064(7), 945(14), 929(14), 827(31), 800(8), 766(3), 748(3), 720(9), 605(6), 548(3), 363(7), 363(7), 339(11), 273(3), 205(7), 156(14), 101(20); ¹H NMR ([D₆]DMSO): δ = 8.59 (s, 6 H), 6.13 ppm (br s, 4 H); ¹³C NMR([D₆]DMSO): δ = 160.8 (s, C₁–O), 152.0 (s, C–NH₂), 141.8 (s, C₄–NO₂), 137.8 (s, C–C), 125.2 (s, C_{2,6}–NO₂), 124.3 ppm (s, C_{3,5}–H); *m/z* (FAB⁻): 228.0 (C₆H₂N₃O₇⁻), *m/z* (FAB⁺): 197.0 (C₄H₉N₁₀⁺); EA (C₁₆H₁₄N₁₆O₁₄, 654.38): C 29.37, H 2.16, N 34.25; found: C 29.36, H 2.24, N 34.03; BAM impact: 30 J, BAM friction: 360 N, ESD: 0.75 J (at grain sizes <100 µm).

2.13. 4,4',5,5'-Tetraamino-3,3'-bi-1,2,4-triazolium dinitroformate (13)

4,4',5,5'-Tetraamino-3,3'-bi-1,2,4-triazole (**1**) (196.2 mg, 1.00 mmol, 1.00 eq.) and trinitromethane (302 mg, 2.00 mmol, 2.00 eq.) were dissolved in 50 mL of water under heating until a clear solution was observed. The solution was stirred for further 30 min and then left for crystallization to give yellow crystals. Yield: 350 mg, 0.70 mmol, 70%.

DTA (5 °C min⁻¹) onset: 94 °C (dec.); IR (ATR, cm⁻¹): $\tilde{\nu}$ = 3435(m), 3315(s), 3249(s), 1690(vs), 1606(m), 1517(s), 1481(s), 1402(s), 1384(m), 1317(m), 1231(vs), 1152(s), 1132(vs), 1078(s), 976(s), 864(s), 780(s), 729(s), 689 (m); Raman (1064 nm, 300 mW, 25 °C, cm⁻¹): $\tilde{\nu}$ = 3328(2), 3277(3), 1650(100), 1608(8), 1559(5), 1517(4), 1467(8), 1449(7), 1386(22), 1353(12), 1294(33), 1277(32), 1255(32), 1163(14), 1146(15), 1059(4), 868(60), 804(17), 785(14), 721(7), 604(4), 472(11), 426(9), 426(9), 381(7), 325(11), 272(10), 172(16), 146(24), 109(33), 81(46); ¹H NMR ([D₆]DMSO): δ = 8.61 (s, 6 H), 6.13 ppm (br s, 4 H); ¹³C NMR([D₆]DMSO): δ = 152.0 (s, C–NH₂), 150.3 (s, C(NO₂)₃), 137.8 ppm(s, C–C); *m/z* (FAB⁻): 150.0 (CN₃O₆⁻), *m/z* (FAB⁺): 197.0 (C₄H₉N₁₀⁺); EA (C₆H₁₀N₁₀O₁₂, 498.24): C 14.46,

H 2.02, N 44.98; found: C 14.54, H 2.03, N 44.95; BAM impact: 4 J, BAM friction: 160 N, ESD: 0.8 J (at grain sizes <100 μm).

3. X-ray Diffraction

3.1. Instrument and refinement software

Suitable single crystal of compounds **1–3**, **5–8**, **11** and **13** were picked from the crystallization mixtures and mounted in Kel-F oil, transferred to the N₂ stream of an Oxford Xcalibur3 diffractometer with a Spellman generator (voltage 50 kV, current 40 mA) and a KappaCCD detector. The data collection was performed using the CRYSTALIS CCD software⁹, the data reduction using the CRYSTALIS RED software¹⁰. The structure was solved with SIR-92¹¹, refined with SHELXL-97¹² and finally checked using the PLATON software¹³ integrated in the WINGX software suite.¹⁴ The non-hydrogen atoms were refined anisotropically and the hydrogen atoms were located and freely refined. The absorptions were corrected using a SCALE3 ABSPACK multi-scan method.¹⁵

3.2. Crystallographic data and refinement parameters

Table S1. Crystallographic data and refinement parameters of compound **2** at different temperatures.

	2 (173K_1)	2 (173K_2)	2 (100K)	2 (298K)
Formula	C ₄ H ₁₀ N ₁₆ O ₈	C ₄ H ₁₀ N ₁₆ O ₈	C ₄ H ₁₀ N ₁₆ O ₈	C ₄ H ₁₀ N ₁₆ O ₈
FW [g mol ⁻¹]	410.28	410.28	410.28	410.28
Crystal system	triclinic	triclinic	triclinic	triclinic
Space Group	<i>P</i> –1	<i>P</i> –1	<i>P</i> –1	<i>P</i> –1
Color / Habit	colorless, plate	colorless, plate	colorless, plate	colorless, plate
Size [mm]	0.03 × 0.10 × 0.20	0.10 × 0.10 × 0.10	0.10 × 0.10 × 0.10	0.10 × 0.10 × 0.10
<i>a</i> [Å]	6.5168(5)	6.5155(8)	6.5046(9)	6.5597(12)
<i>b</i> [Å]	7.7826(5)	7.7748(11)	7.7010(13)	7.984(2)
<i>c</i> [Å]	8.5072(6)	8.5036(11)	8.4831(13)	8.5813(19)
α [°]	97.717(6)	97.677(11)	97.897(13)	97.31(2)
β [°]	107.340(6)	107.306(11)	107.262(13)	107.895(19)
γ [°]	112.140(7)	112.194(12)	111.478(14)	113.84(2)
<i>V</i> [Å ³]	366.35(6)	365.76(10)	362.85(12)	374.52(18)
<i>Z</i>	1	1	1	1
$\rho_{\text{calc.}}$ [g cm ⁻³]	1.860	1.863	1.878	1.819
μ [mm ⁻¹]	0.171	0.171	0.171	0.171
<i>F</i> (000)	210	210	210	210
λ_{MoKa} [Å]	0.71073	0.71073	0.71073	0.71073
T [K]	173	173	100	298
9 min-max [°]	4.4, 26.5	4.4, 26.5	4.5, 26.5	4.4, 26.5
Dataset h; k; l	-8:8; -9:9; -10:10	-4:8; -9:9; -10:9	-4:8; -9:9; -10:9	-4:8; -9:9; -10:9
Reflect. coll.	5373	1997	1969	2030
Independ. refl.	1510	1498	1482	1537
R _{int}	0.026	0.016	0.017	0.017
Reflection obs.	1320	1183	1225	1046
No. parameters	147	147	147	147
<i>R</i> ₁ (obs)	0.0336	0.0402	0.0384	0.0630
w <i>R</i> ₂ (all data)	0.0855	0.1012	0.1013	0.1720
<i>S</i>	1.06	1.06	1.06	1.02
Resd. Dens.[e Å ⁻³]	-0.34, 0.38	-0.25, 0.29	-0.27, 0.26	-0.42, 0.50
Device type	Oxford XCalibur3 CCD	Oxford XCalibur3 CCD	Oxford XCalibur3 CCD	Oxford XCalibur3 CCD
Solution	SIR-2004	SIR-2004	SIR-2004	SIR-2004
Refinement	SHELXL-97	SHELXL-97	SHELXL-97	SHELXL-97
Absorpt. corr.	multi-scan	multi-scan	multi-scan	multi-scan
CCDC	1029064	1035376	1035375	1035377

Table S2. Crystallographic data and refinement parameters of compounds **3–6**.

	3	4	5	6
Formula	C ₆ H ₁₀ N ₂₀ O ₆	C ₆ H ₁₄ N ₂₀ O ₆	C ₄ H ₁₀ N ₁₂ O ₆	C ₁₀ H ₁₀ N ₁₈ O ₈
FW [g mol ⁻¹]	458.34	462.37	322.24	510.36
Crystal system	triclinic	monoclinic	triclinic	monoclinic
Space Group	<i>P</i> –1	<i>P</i> 2 ₁ /c	<i>P</i> –1	<i>P</i> 2 ₁ /c
Color / Habit	colorless, plate	colorless, block	colorless, plate	yellow, plate
Size [mm]	0.05 × 0.14 × 0.28	0.19 × 0.29 × 0.32	0.04 × 0.20 × 0.30	0.02 × 0.06 × 0.10
<i>a</i> [Å]	6.6569(6)	6.2655(3)	6.6825(4)	5.2141(4)
<i>b</i> [Å]	8.3735(8)	8.2526(4)	6.9310(4)	9.8545(6)
<i>c</i> [Å]	8.5943(8)	17.2616(8)	7.0089(5)	17.7329(11)
α [°]	88.177(8)	90	73.212(6)	90
β [°]	68.659(9)	92.655(5)	89.114(6)	98.076(2)
γ [°]	69.429(8)	90	75.819(5)	90
<i>V</i> [Å ³]	415.22(8)	891.58(7)	300.79(4)	902.12(10)
<i>Z</i>	1	2	1	2
$\rho_{\text{calc.}}$ [g cm ⁻³]	1.833	1.722	1.779	1.879
μ [mm ⁻¹]	0.159	0.149	0.160	0.163
<i>F</i> (000)	234	476	166	520
$\lambda_{\text{MoK}\alpha}$ [Å]	0.71073	0.71073	0.71073	0.71073
T [K]	173	173	173	173
9 min-max [°]	4.9, 26.5	4.1, 26.5	4.3, 26.5	2.3, 26.4
Dataset <i>h</i> ; <i>k</i> ; <i>l</i>	–8:8; –10:9; –10:10	–7:7; –10:7; –21:21	–8:8; –8:8; –8:8	–6:6; –12:12; –22:22
Reflect. coll.	3195	6534	4404	23035
Independ. refl.	1718	1834	1242	1845
R _{int}	0.024	0.026	0.024	0.079
Reflection obs.	1381	1594	1086	1391
No. parameters	165	173	120	183
R ₁ (obs)	0.0359	0.0346	0.0313	0.0370
wR ₂ (all data)	0.0913	0.0915	0.0898	0.1108
<i>S</i>	1.07	1.10	1.09	1.11
Resd. Dens.[e Å ⁻³]	–0.23, 0.19	–0.37, 0.29	–0.22, 0.26	–0.28, 0.28
Device type	Oxford XCalibur3 CCD	Oxford XCalibur3 CCD	Oxford XCalibur3 CCD	Oxford XCalibur3 CCD
Solution	SIR-2004	SIR-2004	SIR-2004	SIR-2004
Refinement	SHELXL-97	SHELXL-97	SHELXL-97	SHELXL-97
Absorpt. corr.	multi-scan	multi-scan	multi-scan	multi-scan
CCDC	1029053	1029066	1029061	1029060

Table S3. Crystallographic data and refinement parameters of compounds **7–9**.

	7	7 · 2 H₂O	8	9
Formula	C ₆ H ₁₀ N ₁₈ O ₂	C ₆ H ₁₄ N ₁₈ O ₄	C ₆ H ₁₀ N ₂₂ O ₄	C ₁₀ H ₂₂ N ₃₂ O ₅
FW [g mol ⁻¹]	366.32	402.35	454.36	679.60
Crystal system	triclinic	monoclinic	triclinic	monoclinic
Space Group	<i>P</i> –1	<i>P</i> 2 ₁ /c	<i>P</i> –1	<i>C</i> 2/c
Color / Habit	colorless, block	colorless, needle	colorless, plate	colorless, plate
Size [mm]	0.03 × 0.10 × 0.10	0.03 × 0.03 × 0.13	0.02 × 0.16 × 0.40	0.05 × 0.20 × 0.35
<i>a</i> [Å]	6.3741(7)	8.9220(7)	6.3892(6)	28.2349(8)
<i>b</i> [Å]	7.8143(8)	14.3723(8)	8.2420(7)	12.8429(3)
<i>c</i> [Å]	8.4826(8)	6.7226(6)	8.4392(7)	7.2379(3)
α [°]	66.716(9)	90	81.266(7)	90
β [°]	69.319(9)	110.555(10)	75.251(7)	94.715(3)
γ [°]	76.365(9)	90	85.638(7)	90
<i>V</i> [Å ³]	360.81(7)	806.99(11)	424.46(7)	2615.71(15)
<i>Z</i>	1	2	1	4
$\rho_{\text{calc.}}$ [g cm ⁻³]	1.686	1.656	1.778	1.703
μ [mm ⁻¹]	0.137	0.139	0.150	0.140
<i>F</i> (000)	188	416	232	1384
$\lambda_{\text{MoK}\alpha}$ [Å]	0.71073	0.71073	0.71073	0.71073
T [K]	173	173	173	173
θ min-max [°]	4.2, 26.5	4.3, 26.5	4.1, 26.5	4.3, 26.5
Dataset h; k; l	–7:7; –9:9; –10:10	–11:11; –16:18; –4:8	–8:8 ; –10:10 ; –10:10	–35:35; –16:16 ; –9:9
Reflect. coll.	2719	3575	6245	19744
Independ. refl.	1478	1671	1750	2706
R _{int}	0.030	0.023	0.036	0.032
Reflection obs.	1099	1372	1390	2355
No. parameters	138	155	165	257
R ₁ (obs)	0.0403	0.0356	0.0356	0.0318
wR ₂ (all data)	0.095	0.0801	0.0862	0.0874
<i>S</i>	1.02	1.04	1.02	1.03
Resd. Dens. [e Å ⁻³]	–0.20, 0.23	–0.21, 0.22	–0.27, 0.18	–0.19, 0.24
Device type	Oxford XCalibur3 CCD	Oxford XCalibur3 CCD	Oxford XCalibur3 CCD	Oxford XCalibur3 CCD
Solution	SIR-2004	SIR-2004	SIR-2004	SIR-2004
Refinement	SHELXL-97	SHELXL-97	SHELXL-97	SHELXL-97
Absorpt. corr.	multi-scan	multi-scan	multi-scan	multi-scan
CCDC	1029062	1029063	1029058	1029056

Table S4. Crystallographic data and refinement parameters of compounds **9a–10** and **13**.

	9a	9b	10	13
Formula	C ₁₆ H ₃₆ N ₅₄ O ₁₀	C ₁₀ H ₂₈ N ₃₂ O ₈	C ₈ H ₂₀ N ₂₂ O ₆	C ₆ H ₁₀ N ₁₆ O ₁₂
FW [g mol ⁻¹]	1144.99	724.64	520.46	498.24
Crystal system	monoclinic	triclinic	triclinic	monoclinic
Space Group	<i>P</i> 2 ₁ / <i>c</i>	<i>P</i> —1	<i>P</i> —1	<i>P</i> 2 ₁ / <i>c</i>
Color / Habit	colorless, stab	colorless block	colorless, block	colorless, plate
Size [mm]	0.11 × 0.12 × 0.31	0.38 × 0.40 × 0.40	0.35 × 0.21 × 0.14	0.32 × 0.27 × 0.03
<i>a</i> [Å]	10.9541(3)	9.2750(7)	6.4916(3)	16.8271(4)
<i>b</i> [Å]	19.7090(4)	9.5238(8)	7.9296(4)	12.0361(3)
<i>c</i> [Å]	20.4037(7)	9.8392(8)	10.1535(5)	8.7485(3)
α [°]	90	109.650(7)	87.069(4)	90
β [°]	104.295(3)	96.080(6)	77.437(4)	93.252(2)
γ [°]	90	116.486(8)	84.279(4)	90
<i>V</i> [Å ³]	4268.7(2)	698.14(13)	507.37(4)	1769.00(9)
<i>Z</i>	4	1	1	4
$\rho_{\text{calc.}}$ [g cm ⁻³]	1.782	1.724	1.703	1.871
μ [mm ⁻¹]	0.149	0.146	0.144	0.176
<i>F</i> (000)	2360	376	270	1016
$\lambda_{\text{MoK}\alpha}$ [Å]	0.71073	0.71073	0.71073	0.71073
T [K]	173	173	173	173
9 min-max [°]	4.1, 26.5	4.2, 26.5	4.1, 26.5	4.2, 26.5
Dataset h; k; l	−13:13; −22:24; −25:22	−11:11; −11:11; −11:12	−8:8; −9:9; −12:12	−21:21; −15:15; −10:10
Reflect. coll.	22613	5502	7429	26371
Independ. refl.	8801	2872	2089	3649
R _{int}	0.025	0.019	0.019	0.030
Reflection obs.	6673	2371	1909	3154
No. parameters	865	282	203	347
R ₁ (obs)	0.0376	0.0328	0.0302	0.0299
wR ₂ (all data)	0.0990	0.0874	0.0764	0.0778
<i>S</i>	1.03	1.02	1.08	1.05
Resd. Dens.[e Å ⁻³]	−0.26, 0.33	−0.24, 0.30	−0.26, 0.26	−0.26, 0.21
Device type	Oxford XCalibur3 CCD	Oxford XCalibur3 CCD	Oxford XCalibur3 CCD	Oxford XCalibur3 CCD
Solution	SIR-2004	SIR-2004	SIR-2004	SIR-2004
Refinement	SHELXL-97	SHELXL-97	SHELXL-97	SHELXL-97
Absorpt. corr.	multi-scan	multi-scan	multi-scan	multi-scan
CCDC	1029055	1029057	1029054	1029059

3.3. Crystal structures of compounds 4, 7 · 2 H₂O, 9–10 and 13

3.3.1. 4,4',5,5'-Tetraamino-3,3'-bi-1,2,4-triazolium nitrotetrazolate dihydrate (4)

The energetic salt 4,4',5,5'-tetraamino-3,3'-bi-1,2,4-triazolium nitro-tetrazolate crystallizes from water in the monoclinic space group $P2_1/c$ with two water moieties and two molecules per unit cell. The torsion angle of N1–C1–C1ⁱ–N3ⁱ is equal to 0.6(2) $^\circ$ yielding a planar structure. The molecular unit of compound **4** is illustrated in Figure S1.

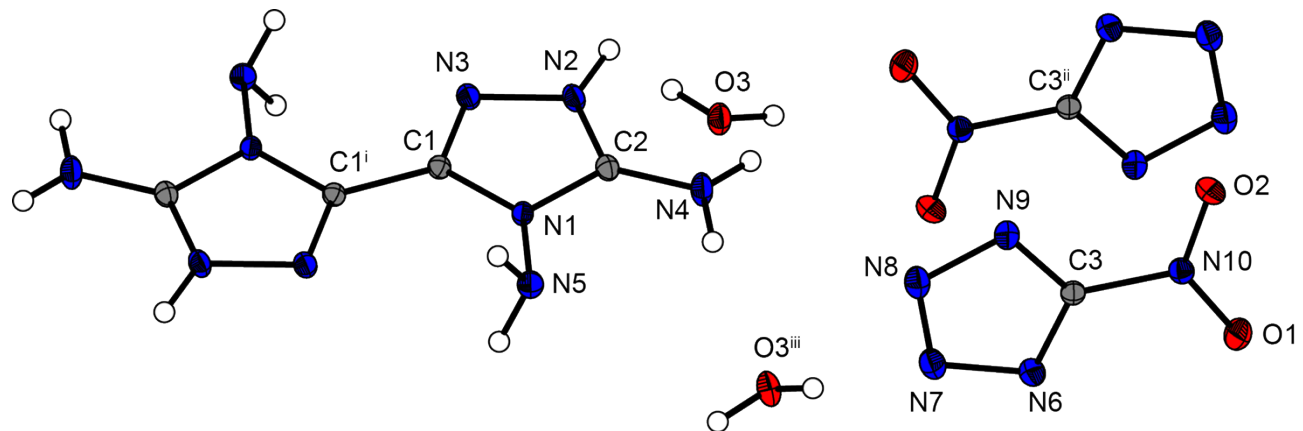


Figure S1. Molecular unit of **4**. Ellipsoids are drawn at the 50% probability level. Selected bond lengths [Å]: C1–C1ⁱ 1.446(9), C2–N4 1.315(8), C3–N10 1.444(9).

3.3.2. 4,4',5,5'-Tetraamino-3,3'-bi-1,2,4-triazolium bistetrazolate-1-oxide dihydrate (7 · 2 H₂O)

The energetic salt **7** crystallizes from water as water free structure and as a dihydrate (**7 · 2 H₂O**) in the monoclinic space group $P2_1/c$ with two water moieties and two molecules per unit cell. The molecular unit of compound **7 · 2 H₂O** is illustrated in Figure S2.

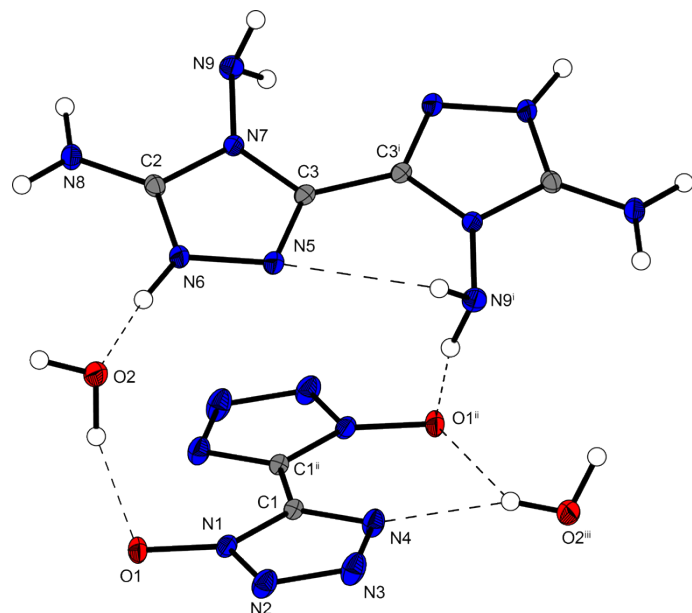


Figure S2. Molecular unit of $7 \cdot 2 \text{ H}_2\text{O}$. Ellipsoids are drawn at the 50% probability level.

3.3.3. 4,4',5,5'-Tetraamino-3,3'-bi-1,2,4-triazolium 5-nitrimino-1*H*-tetrazolate hemihydrate (**9**)

4,4',5,5'-Tetraamino-3,3'-bi-1,2,4-triazolium 5-nitrimino-1*H*-tetrazolate hemihydrate (**9**) crystallizes in a stoichiometric composition of 1:1 in the monoclinic space group *C*2/*c* with 0.5 moieties of water per unit cell. The density of compound **9** at 173 K amounts to 1.703 g cm⁻³ and thus exhibits the exact same density as the 1-methyl derivative **10**. Energetic nitriminotetrazolates, as the hydroxylammonium salt with a density 1.785 g cm⁻³ or the hydrazinium salt with a lower density of 1.635 g cm⁻³,¹⁶ show very different densities. Since compound **9** crystallizes with crystal water, the comparison of the densities is just a rough point of reference. The cation forms a planar system with a torsion angle of N9–C2–C4–N12 equal to 0.5(2)°. The bond length of C1 to the N5 of the nitrimino-group is similar to the lengths of similar salts reported in literature.¹⁶ The molecular unit of compound **9** is illustrated in Figure S3.

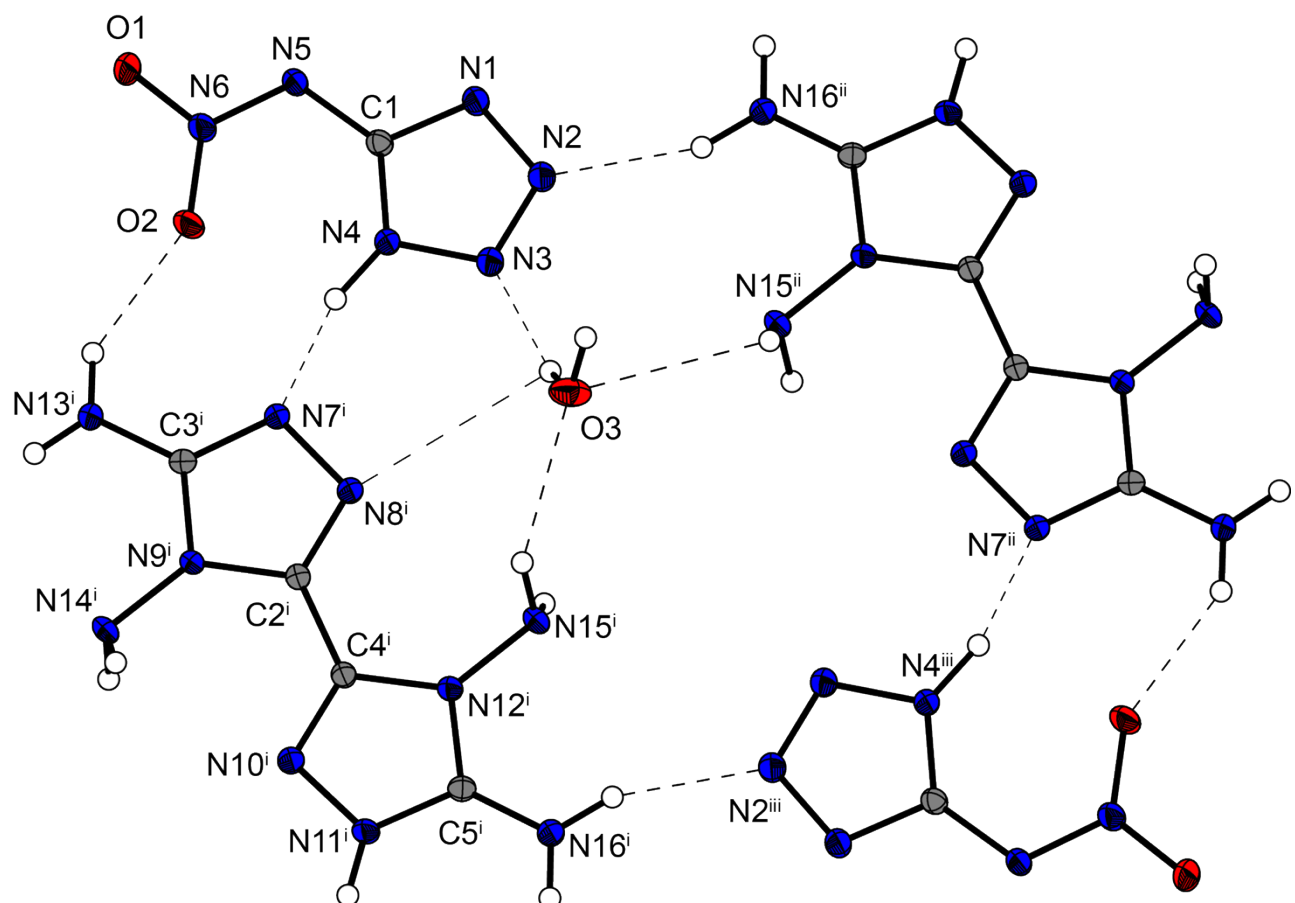


Figure S3. Molecular structure of **9**. Ellipsoids are drawn at the 50% probability level.

Selected bond lengths [Å]: C2–C4ⁱ 1.445(8), C5ⁱ–N16ⁱ 1.313(6) C1–N5 1.370(1); selected torsion angle [°]: N9–C2–C4–N12 0.5(2).

Further crystal structures of the 5-nitriminotetrazolate salt were obtained (**9a** and **9b**) and are displayed in Figures S4 and S5

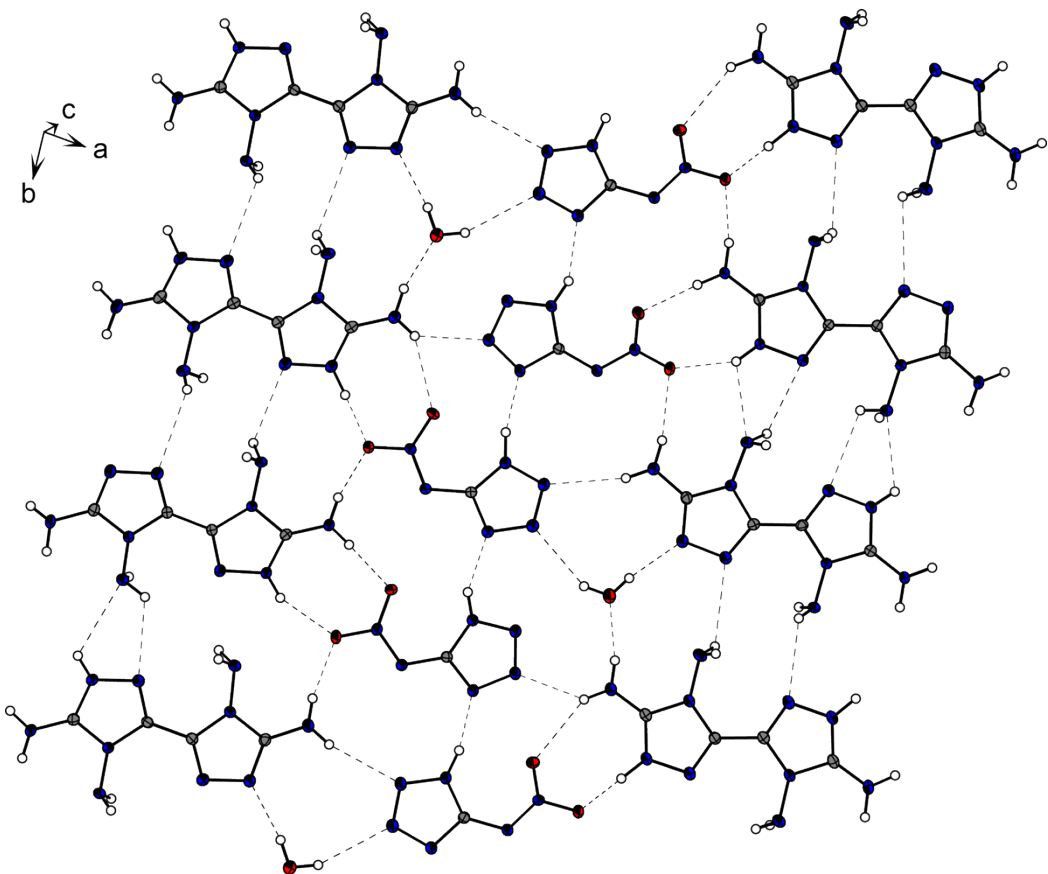


Figure S4. Structure of **9a**. Ellipsoids are drawn at the 50% probability level.

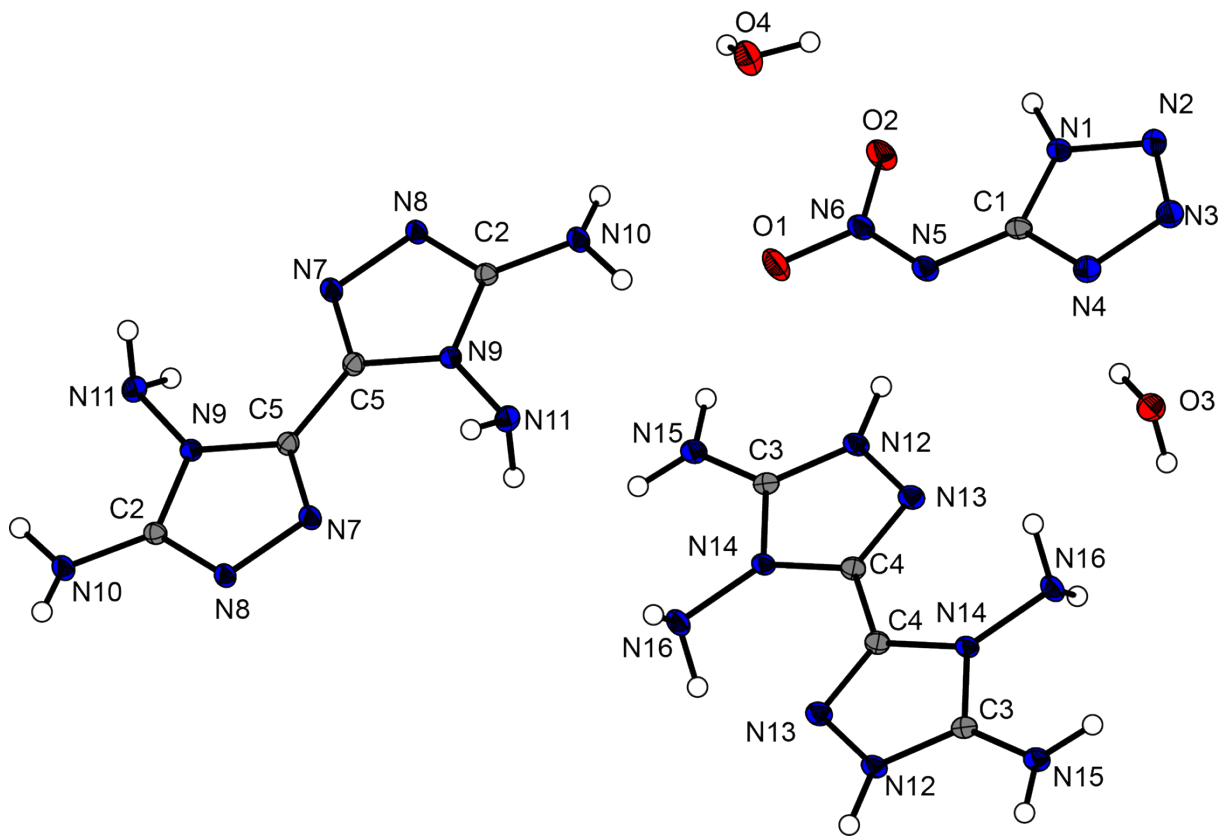


Figure S5. Structure of **9b**. Ellipsoids are drawn at the 50% probability level.

3.3.4. 4,4',5,5'-Tetraamino-3,3'-bi-1,2,4-triazolium 1-methyl-5-nitriminotetrazolate dihydrate (10)

The energetic compound 4,4',5,5'-tetraamino-3,3'-bi-1,2,4-triazolium 1-methyl-5-nitriminotetrazolate crystallizes from water in the triclinic space group $P\bar{1}$ with two water moieties and a density of 1.703 g cm^{-3} at 173 K. The bond length C3–N10 corresponds more to the length of a C=N double bond and is similar to the length of reported 1-methylnitriminotetrazoles.¹⁷ The molecular unit of compound **10** is illustrated in Figure S6.

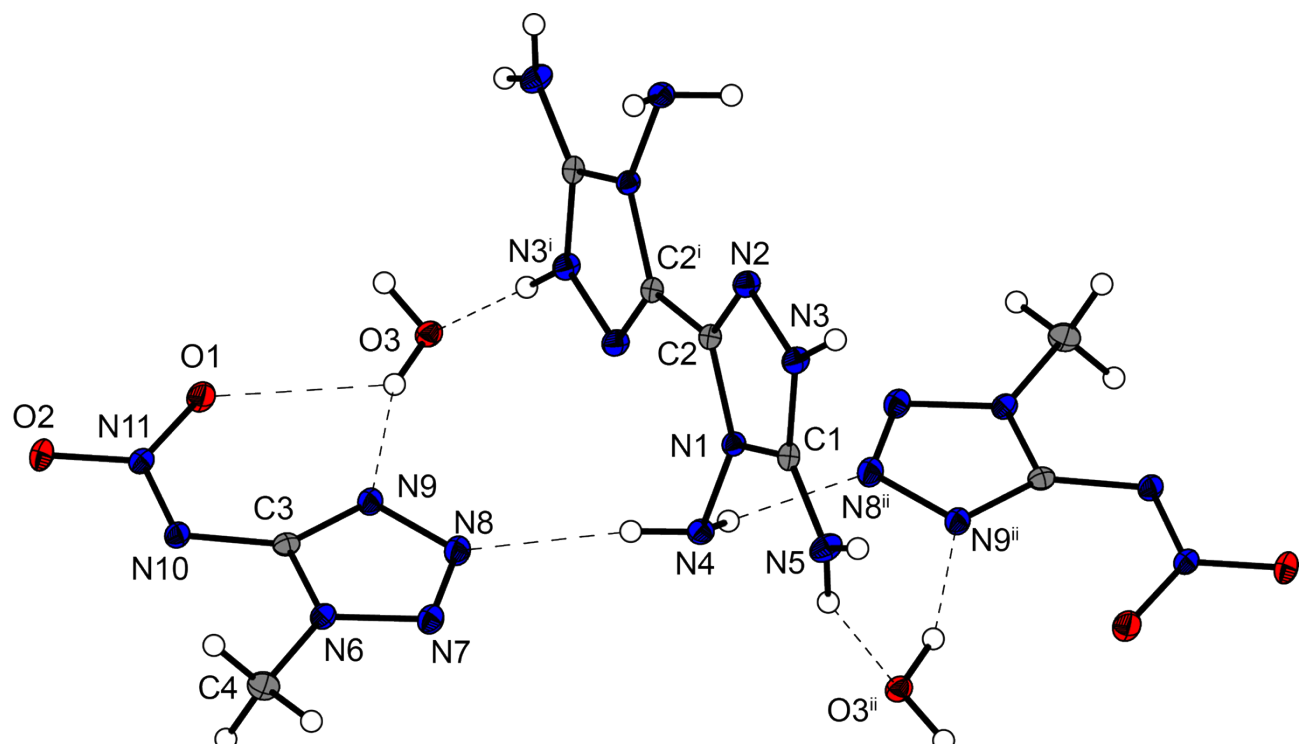


Figure S6. Molecular unit of **10**. Ellipsoids are drawn at the 50% probability level. Selected bond lengths [\AA]: C2–C2ⁱ 1.451(2), C1–N5 1.321(1), C3–N10 1.376(0); selected hydrogen–bridge–bond–lengths [\AA]: O3–H3B–O1 1.97, O3–H3B–O2 2.63(2), O3–H3A–O1 2.45(2).

3.3.5. 4,4',5,5'-Tetraamino-3,3'-bi-1,2,4-triazolium dinitroformate (13)

4,4',5,5'-Tetraamino-3,3'-bi-1,2,4-triazolium dinitroformate (**13**) crystallizes in the monoclinic space group $P2_1/c$ with a density of 1.871 g cm^{-3} at 173 K. The molecular unit of compound **13** is illustrated in Figure S7.

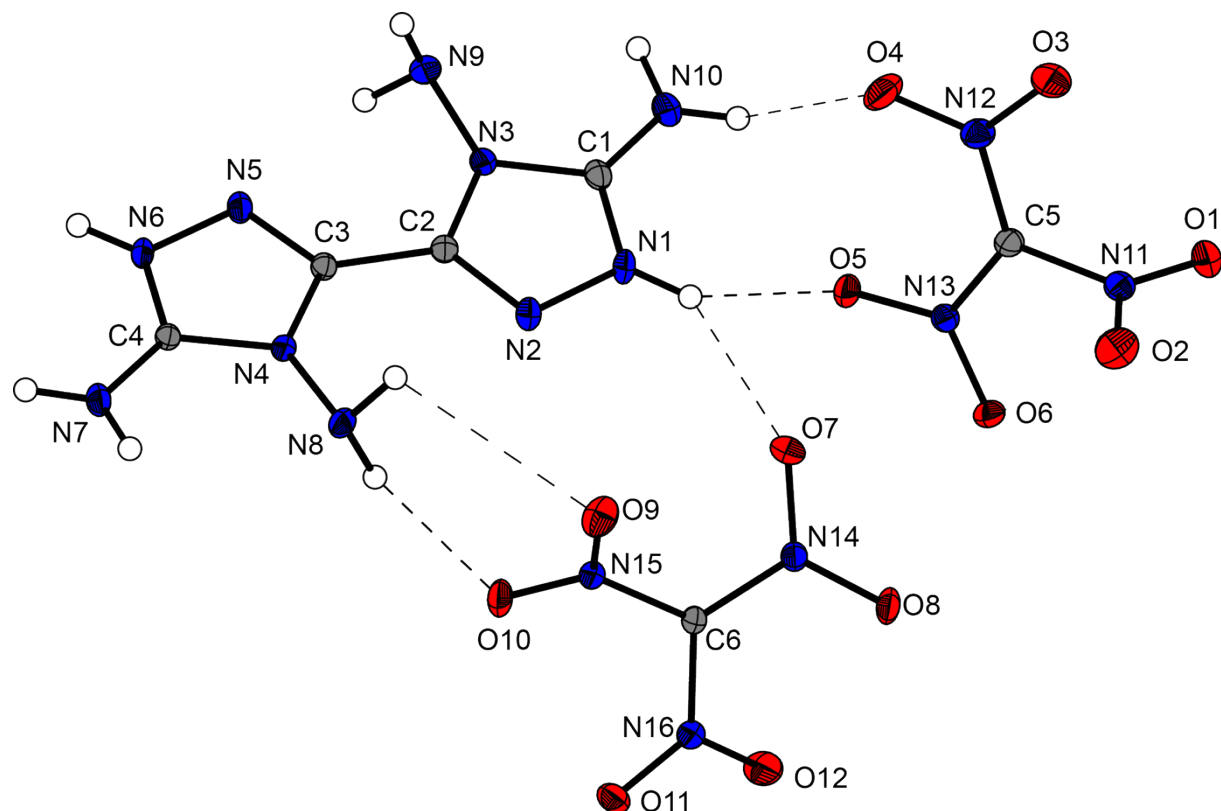


Figure S7. Molecular structure of **13**. Ellipsoids are drawn at the 50% probability level.

4. Electron Microscopy

First morphological investigations of compound **2** were carried out on a JSM-6500F scanning electron microscope (SEM) (JEOL Ltd., Tokyo, Japan) with a field emission source operated at 4.0 to 12.0 kV. All images shown are secondary electron images in the Figures S8a–S8d. The average chemical composition was studied with an energy-dispersive X-ray spectrometry (EDS) detector model 7418 (Oxford instruments, Oxfordshire, UK). Powders were placed on a brass sample carrier fixed with self-adhesive carbon plates (Plano, Wetzlar, Germany). The samples were sputtered with carbon (sputter device: BAL-TEC MED 020, BAL-TEC AG, Balzers, Netherlands) before loading them into the SEM chamber, since the reaction products were not electrically conducting.

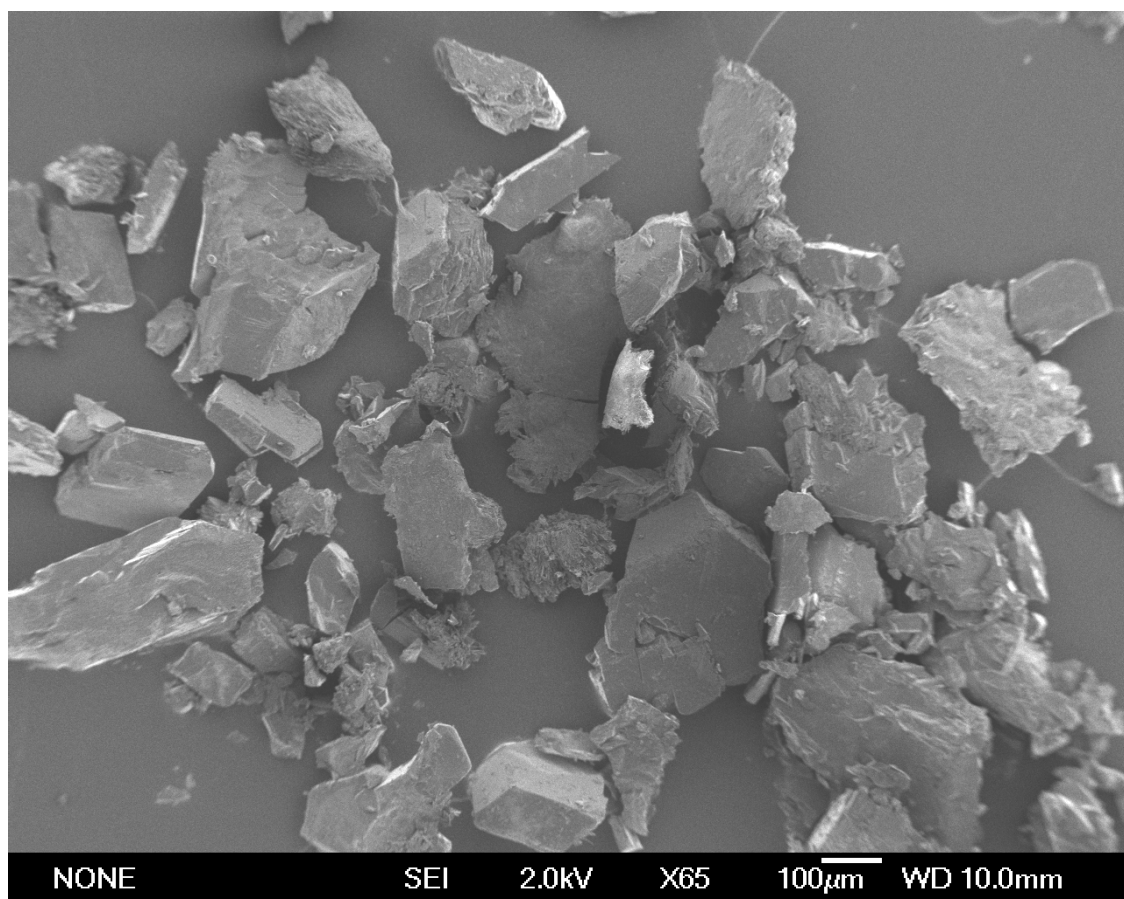


Figure S8a. Morphology of compound **2**.

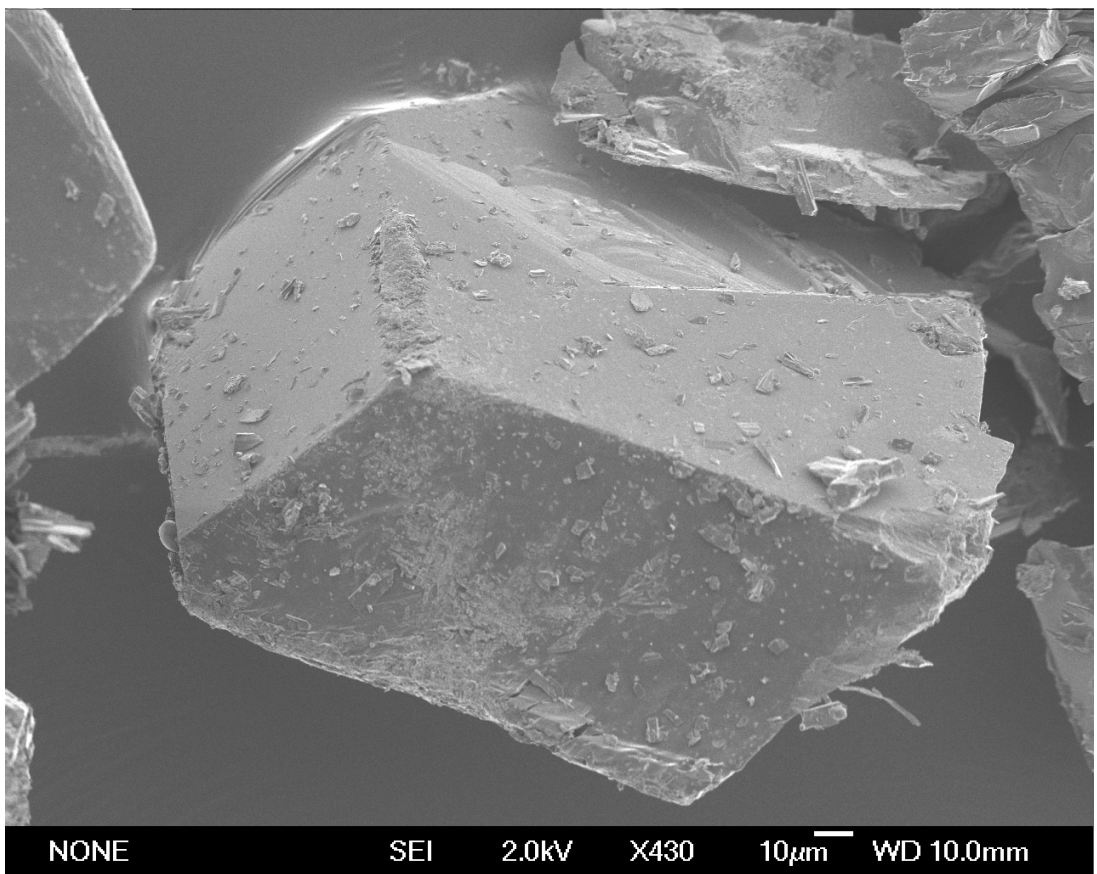


Figure S8b. Morphology of compound 2.

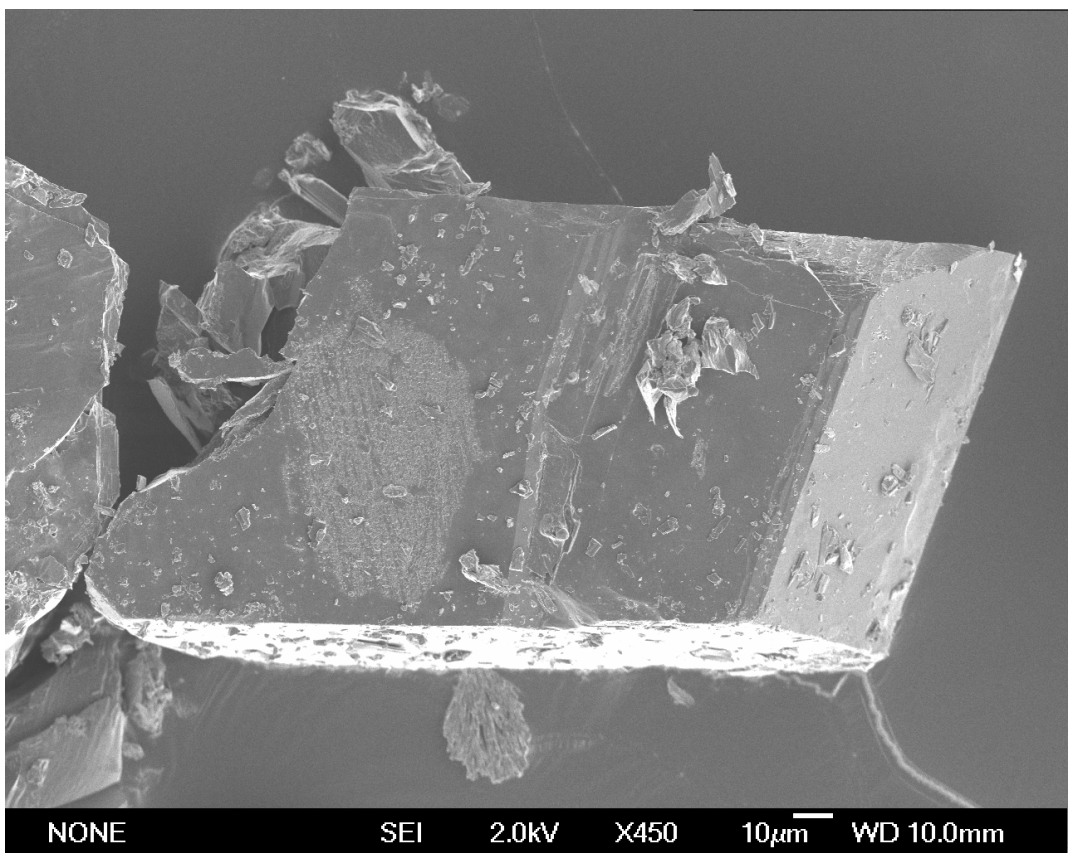


Figure S8c. Morphology of compound 2.

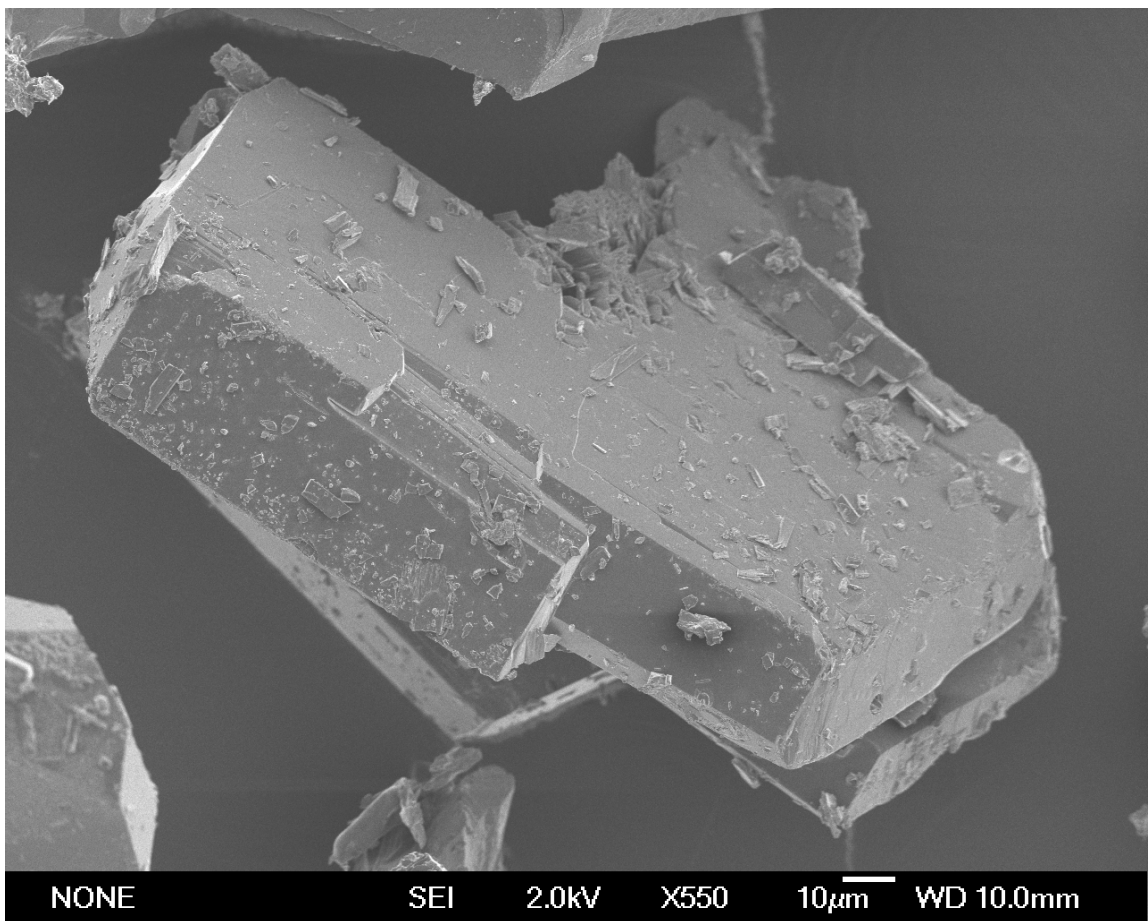


Figure S8d. Morphology of compound 2.

5. Explosive performance

5.1. Heat of formation calculations

Heats of formation of compounds **1–3**, **5–8**, **11** and **13** were calculated using the atomization method (equation S1) using room temperature CBS-4M enthalpies summarized in Table S5.^{18,19}

$$\Delta_f H^\circ_{(g, M, 298)} = H_{(\text{Molecule}, 298)} - \sum H^\circ_{(\text{Atoms}, 298)} + \sum \Delta_f H^\circ_{(\text{Atoms}, 298)} \quad (\text{S1})$$

Table S5 CBS-4M electronic enthalpies for atoms C, H, N and O and their literature values for atomic $\Delta H^\circ_f{}^{298}$ / kJ mol⁻¹

	$-H^{298}$ / a.u.	NIST ²⁰
H	0.500991	218.2
C	37.786156	717.2
N	54.522462	473.1
O	74.991202	249.5

Quantum chemical calculations were carried out using the Gaussian G09 program package. The enthalpies (H) and free energies (G) were calculated using the complete basis set (CBS) method of Petersson and coworkers in order to obtain very accurate energies. The CBS models use the known asymptotic convergence of pair natural orbital expressions to extrapolate from calculations using a finite basis set to the estimated CBS limit. CBS-4 begins with an HF/3-21G(d) geometry optimization; the zero point energy is computed at the same level. It then uses a large basis set SCF calculation as a base energy, and an MP2/6- 31+G calculation with a CBS extrapolation to correct the energy through second order. An MP4(SDQ)/6-31+ (d,p) calculation is used to approximate higher order contributions. In this study, we applied the modified CBS.

For neutral **1** the sublimation enthalpy, which is needed to convert the gas phase enthalpy of formation to the solid state one, was calculated by the *Trotton* rule. In the case of the ionic compounds, the lattice energy (U_L) and lattice enthalpy (ΔH_L) were calculated from the corresponding X-ray molecular volumes according to the equations provided by *Jenkins* and *Glasser*.²³ With the calculated lattice enthalpy the gas-phase enthalpy of formation was converted into the solid state (standard conditions) enthalpy of formation. These molar

standard enthalpies of formation (ΔH_m) were used to calculate the molar solid state energies of formation (ΔU_m) according to equation S2.

$$\Delta U_m = \Delta H_m - \Delta n RT \quad (\text{S2})$$

(Δn being the change of moles of gaseous components)

Table S6 Calculation results

M	$-H^{298}$ [a] / a.u.	$\Delta_f H^\circ(g, M)$ / kJ mol ⁻¹ [b]	V_M / nm ³ [c]	ΔU_L (4); ^[d]	ΔH_L ΔH_{sub} [e] (3) / kJ mol ⁻¹	$\Delta_f H^\circ(s)$ [f] / kJ mol ⁻¹	Δn [g]	$\Delta_f U(s)$ [f] / kJ kg ⁻¹
BDAT	703.707615	587.6		115.6		472.0	9.0	2520.3
BDAT²⁺	704.327388	2032.9						
DN⁻	464.499549	-124.0						
BDAT²⁺ DN⁻		1787.5	0.373	1478.5, 1485.9	301.5		17	837.7
NT2O⁻	536.798772	83.0						
BDAT NT2O		2201.6	0.423	1433.0, 1440.4	761.2		18	1758.3
NO₃⁻	280.080446	-313.6						
BDAT²⁺ (NO₃⁻)₂		1408.3	0.306	1554.0, 1561.5	-153.2		14	-367.7
TNBI²⁻	1266.677508	-33.9						
BDAT²⁺ TNBI²⁻		1760.0	0.460	1658.7, 1672.6	87.3		18	258.6
BT1O²⁻	663.703743	587.7						
BDAT²⁺ BT1O²⁻		2381.6	0.368	1769.8, 1783.7	597.9		15	1733.7
DNABT²⁻	1032.612357							
BDAT DNABT²⁻		2768.8	0.432	1656.2, 1661.1	1107.7		18.0	2536.6
CIO₄⁻	760.171182	-278.2						
BDAT²⁺ (CIO₄⁻)₂		1476.5	0.359	1492.2, 1499.6	-23.1		15.0	35.4
C(NO₂)₃⁻	652.767406	-220.9						
BDAT C(NO₂)₃⁻		1591.1	0.451	141.2, 1417.7	173.4		19.0	442.7

[a] CBS-4M electronic enthalpy; [b] gas phase enthalpy of formation; [c] molecular volumes taken from X-ray structures and corrected to room temperature; [d] lattice energy and enthalpy (calculated using Jenkins and Glasser equations); [e] enthalpy of sublimation (calculated by Trouton rule); [f] standard solid state enthalpy of formation; [g] solid state energy of formation.

5.2. Energetic Performance

In comparison to other reported nitrotetrazolate-2*N*-oxides, the heat of formation of salt **3** (761 kJ mol^{-1}) is exceptionally high, since the highest heat of formation is exhibited by the triaminoguanidinium nitrotetrazolate-2*N*-oxide ($471.5 \text{ kJ mol}^{-1}$), the ammonium salt reaches as low as $152.0 \text{ kJ mol}^{-1}$.²⁴ The value for the high energetic hydroxylammonium salt lies between these two heats of formation ($\Delta_f H_m^\circ = 218.7 \text{ kJ mol}^{-1}$). The nitrate **5** shows a negative heat of formation of $-153.2 \text{ kJ mol}^{-1}$. The nitrogen-rich ammonium and hydroxylammonium nitrates show smaller values with $-365.5 \text{ kJ mol}^{-1}$ ²⁵ and $-364.3 \text{ kJ mol}^{-1}$ ²⁶ in comparison to compound **5**. Compound **6** reveals a heat of formation of 20.9 kJ mol^{-1} . In comparison to the values reported for the aminoguanidinium ($171.1 \text{ kJ mol}^{-1}$), diaminoguanidinium ($399.3 \text{ kJ mol}^{-1}$) and triaminoguanidinium salts ($638.7 \text{ kJ mol}^{-1}$) this value is surprisingly small.²⁷ The 5,5'-bitetrazole-1,1'-dioxide **7** shows a much higher heat of formation of $597.4 \text{ kJ mol}^{-1}$ lying slightly under the heats of formation of the corresponding hydrazinium and aminoguanidinium salts with of $677.7 \text{ kJ mol}^{-1}$ and $668.6 \text{ kJ mol}^{-1}$.²⁸ Other reported salts, like the ammonium or the guanidinium salts, as well as RDX show much smaller heats of formation.²⁸ The highest heat of formation in this report is exhibited by compound **8** with $1107.7 \text{ kJ mol}^{-1}$. This value not only exceeds the value of K₂DNABT ($326.4 \text{ kJ mol}^{-1}$) but also the heat of formation of RDX by far.²⁹ The perchlorate **11** reveals a slightly negative heat of formation of $-23.1 \text{ kJ mol}^{-1}$, whereas the hydroxyammonium perchlorate has a much higher negative heat of formation of $-277.0 \text{ kJ mol}^{-1}$.³⁰

Compound **6** exhibits a detonation velocity of 8237 m s^{-1} and a detonation pressure of 260 kbar thus located within the range of previously reported TNBI salts.²⁷ The hydroxylammonium ($p_{C-J} = 311 \text{ kbar}$, $D = 8362 \text{ m s}^{-1}$), the diaminoguanidinium ($p_{C-J} = 286 \text{ kbar}$, $D = 8377 \text{ m s}^{-1}$) and the triaminoguanidinium salts ($p_{C-J} = 281 \text{ kbar}$, $D = 8388 \text{ m s}^{-1}$) show slightly higher detonation parameters, whereas the guanidinium ($p_{C-J} = 266 \text{ kbar}$, $D = 8070 \text{ m s}^{-1}$) and the aminoguanidinium salts ($p_{C-J} = 268 \text{ kbar}$, $D = 8138 \text{ m s}^{-1}$) show lower detonation velocities and detonation pressures in the same range as compound **6**.²⁷ Compared to compound **7**, other 5,5'-bitetrazole-1,1'-dioxide all show equal if not much larger detonation pressures and velocities than compound **7**.^[27] Only the corresponding guanidiunium, aminoguanidinium and triaminoguanidinium salts with detonation pressures of 233 kbar , 243 kbar and 246 kbar as well as with detonation velocities of 7917 m s^{-1} , 8111 m s^{-1} and 8028 m s^{-1} respectively are in the range of the parameters of compound **7**.²⁸ In comparison the high performance hydroxylammonium salt has a significantly higher detonation pressure of 331 kbar and a fairly higher detonation velocity of 8764 m s^{-1} .²⁸ The

detonation pressure of salt **8** (288 kbar) is lower compared to RDX and with 8804 m s^{-1} the detonation velocity is in the range of RDX. Compared to the potassium salt K₂DNABT, the velocity is much higher (8330 m s^{-1}), whereas the detonation pressure of the potassium salt is a little higher (317 kbar).²⁹ The perchlorate **11** with a detonation velocity of 8290 m s^{-1} and a detonation pressure of 299 kbar.

5.3. Small scale shock reactivity test

The Small-Scale Shock Reactivity Test (SSRT)^{31,32} was introduced by researchers at IHDIV, DSWC (Indian Head Division, Naval Surface Warfare Center). The SSRT measures the shock reactivity (explosiveness) of energetic materials, often well-below critical diameter, without requiring a transition to detonation. The test setup combines the benefits from a lead block test³³ and a gap test.³⁴ In comparison to gap tests, the advantage is the use of a much smaller sample size of the tested explosive (ca. 500 mg). The sample volume V_s is recommended to be 0.284 mL (284 mm^3). For our test setup no possible attenuator (between detonator and sample) and air gap (between sample and aluminum block) was used. The used sample weight m_s was calculated using the formula $V_s \times \rho_{\text{xray}} \times 0.95$. The dent sizes (see Figure S9) were measured by filling them with powdered SiO₂ and measuring the resulting weight.



Figure S9. Aluminum block of the SSRT before (left) and after (right) detonation of dinitramide **2**.

6. Toxicity assessment

The *Luminescent Bacteria Inhibition Test* offers a possibility to determine the environmental acceptability of new energetic materials to aquatic organisms whereat a marine bacteria is used as a representative for marine organisms. In this test the decrease of the luminescence of the liquid-dried bacteria is determined after 15 min and 30 min at different concentrations of the test compounds and is compared to a control measurement of a 2% NaCl stock solution.

The sample dilution sequence corresponds to DIN 38412 L34, which ranges from 1:2 to 1:32 dilution of the compound in the test system. For a better reproducibility, all dilution steps were made in duplicate. The change of intensity of bacterial luminescence in the absence (controls) and in the presence (samples) of the tested substances after different incubation times (15 min, 30 min) were recorded. The controls (2% NaCl only) were measured for calculating the correction factor, which is necessary to consider the normal decrease of luminescence without any toxic effect per time.

The EC₅₀ value gives the concentration of each compound where the bacterial luminescence is inhibited by 50% and is calculated by plotting Γ against the concentration of the test substance in a diagram with a logarithmic scale, where Γ = inhibition (in %) / 100 – inhibition (in %) and c = concentration of the test sample. The EC₅₀ value is identical with the intersection of the resulting graph with the X-axis (Γ = 0).

For better comparison of the resulting toxicities, we also determined the toxic effect of RDX and FOX-12 to the bacterial strain under the same conditions applied for the toxicity assessment of nitramide **2**. To imitate the natural environment of the employed marine bacterium as good as possible, the samples need to be diluted with a 2% (w/v) sodium chloride solution. Since RDX is barely soluble in water, a stock solution in acetone was prepared, which was further diluted with the sodium chloride solution to a mixture containing 200 ppm RDX in water/acetone 99/1 (v/v).

7. Spectroscopy

7.1. NMR Spectroscopy

The peak observed in the ^{13}C -NMR spectrum of compound **3** at 157.4 ppm belongs to the nitrotetrazolate- $2N$ -oxide anion. This chemical shift is very similar to the ones observed in the guanidinium salt (157.6 ppm) or the triaminoguanidinium salt (157.1 ppm) for the carbon of the nitrotetrazolate- $2N$ -oxide.²⁴ The carbon-peak of the nitrotetrazolate anion in compound **4** appears at 168.8 ppm and is only slightly downshifted in comparison to chemical shifts in other nitrogen-rich nitrotetrazolates with chemical shifts between 169.5 and 169.0 ppm.³⁵ The tetranitrobisimidazolate anion in compound **6** exhibits two peaks representing six carbon-atoms in the ^{13}C NMR spectrum at 141.7 (C-C) and 139.4 (C=C) due to the high symmetry of the anion. Depending on the cation, the comparable nitrogenous salts show a very different peak distribution making a comparison between the energetic compounds difficult.³⁶ The peak of the carbons of the 5,5'-bitetrazole-1,1'-dioxide anion of compound **7** appear at 135.2 ppm in the ^{13}C NMR spectrum, thus lying in the range of other reported nitrogen-cations, like the bis(guanidinium) salt (134.6 ppm) or the dihydrazinium salt with a chemical shift of 134.9 ppm.²⁸ The free acid 1*H*,1*H*-5,5-bitetrazole-1,1-diol dihydrate also shows a very similar chemical shift of 135.8 ppm.²⁸ The peaks of the carbons of the anion in compound **8** appear at 140.5 ppm. In comparison to the 5-nitrimino-1*H*-tetrazolate of compound **9** with a chemical shift of the carbon of 157.7 ppm, the 1-methyl derivative **10** shows a chemical shift of the carbon, which amounts to 155.4 ppm. This downshift probably arises through the inductive effect of the methyl-group, pushing electron density into the ring. The carbon-signal of the methyl-group is observed at 32.9 ppm, so that the chemical shift of both peaks lies in the range of the chemical shifts of the 1-methylnitrimotetrazolate-carbons in other nitrogenous compounds, which equal to 157.7 and 33.1 ppm.¹⁷ The picric acid anion in compound **12** leads to four additional peaks in the ^{13}C NMR spectrum, which show similar chemical shifts compared to the shifts of picric acid.³⁷

7.2. IR and Raman Spectroscopy

For the dinitramide anion in compound **2** $\nu(\text{NO}_2)$ is observed at 1532 and 1339 cm^{-1} in the Raman spectrum as well as at similar values in the IR spectrum according to the values reported in literature.³⁸ In the IR and Raman spectra of compounds **3** and **4** a number of bands

occur in the range of 1540–700 cm⁻¹, which show the characteristic pattern of $\nu(\text{NN})$, $\nu(\text{NCN})$, $\gamma(\text{CN})$ and δ aromatic ring vibrations of the tetrazole and the tetrazole–2*N*–oxide rings.³⁵ Additionally the O–H band of the crystal water in compound **4** can be observed at 3106 cm⁻¹. The nitrate anion in compound **5** can be easily identified through a distinct band at 1406 cm⁻¹ in the IR spectrum, showing the valence vibration. The C–NO₂ stretch of the anion of compound **6** can be observed with a very strong band at 1550 cm⁻¹ and medium band at 1351 cm⁻¹ in the Raman spectrum. These bands can also be observed with reversed intensities in the IR spectrum. The usually strongest aromatic C=C stretch band can be observed in the IR spectrum at 1497 cm⁻¹. The characteristic C–C stretch probably overlaps with the C–C stretch of the cation and thus only a single band is observed for the two vibrations at 1024 cm⁻¹. The tetrazole derivatives in compounds **7**, **8**, **9** and **10** show similar absorption patterns in the range of 1540 to 700 cm⁻¹ compared to the ones observed for compound **3** and **4** for the tetrazole–rings. The C–C absorption of compound **7** and **8** occurs at 1001 and 993 cm⁻¹, thus in the range of the C–C band of the cation, so that the two bands probably overlap. Compounds **7**, **8** and **9** all exhibit a weak band at around 1530 cm⁻¹ in both IR and Raman spectra representing the NO₂ stretch of the nitrimino–group. In compound **10** this absorption seems to be shifted to around 1500 cm⁻¹ in the vibrational spectra. Characteristic for the anion in compound **10** are the bands of the –CH₃ group at around 2900 cm⁻¹ (broad band), 1468 cm⁻¹ (δ C–H), 1400 cm⁻¹ (symmetric deformation vibration of CH₃). The absorption at 3360 cm⁻¹ indicates the presence of crystal water in compound **10**. The presence of the perchlorate anion in compound **11** is indicated by the bands at 929, 1075 and 1138 cm⁻¹ in the Raman spectrum. These bands correlate in reasonable agreement with the bands reported for inorganic perchlorate compounds.³⁸ In the vibrational spectra of compound **12** the characteristic vibrations of the C=C stretch vibrations of the aromatic ring can be observed at 1616, 1565 and 1520 cm⁻¹ and thus stand in good agreement to the values reported in literature.³⁹ The C–NO₂ stretch can be observed in the Raman spectra at 1545 and 1368 cm⁻¹. Lastly the characteristic C–O stretch vibration occurs in both IR and Raman spectra between 1150 and 1040 cm⁻¹.

8. References

- 1 NATO standardization agreement (STANAG) on explosives. *Impact sensitivity tests*. No. 4489, 1st ed., Sept. 17, 1999.
- 2 WIWEB-Standardarbeitsanweisung 4-5.1.02, Ermittlung der Explosionsgefährlichkeit, hier der Schlagempfindlichkeit mit dem Fallhammer, Nov. 8, 2002.

- 3 <http://www.bam.de>
- 4 NATO standardization agreement (STANAG) on explosive. *Friction sensitivity tests*. No. 4487, 1st ed., Aug. 22, 2002.
- 5 WIWEB-Standardarbeitsanweisung 4-5.1.03, Ermittlung der Explosionsgefährlichkeit oder der Reibeempfindlichkeit mit dem Reibeapparat, Nov. 8, 2002.
- 6 Impact: Insensitive > 40 J, less sensitive ≥ 35 J, sensitive ≥ 4 J, very sensitive ≤ 3 J; friction: Insensitive > 360 N, less sensitive = 360 N, sensitive < 360 N a. > 80 N, very sensitive ≤ 80 N, extreme sensitive ≤ 10 N; according to the UN recommendations on the transport of dangerous goods. (+) Indicates: not safe for transport.
- 7 <http://www.ozm.cz>
- 8 R. Centore, A. Carella, S. Fusco, *Struct. Chem.* **2011**, *22*, 1095–1103.
- 9 CrysAlis CCD, Oxford Diffraction Ltd., Version 1.171.27p5 beta (release 01-04-2005 CrysAlis171.NET) (compiled Apr 1 2005,17:53:34).
- 10 CrysAlis RED, Oxford Diffraction Ltd., Version 1.171.27p5 beta (release 01-04-2005 CrysAlis171.NET) (compiled Apr 1 2005,17:53:34).
- 11 Altomare, A.; Cascarano, G.; Giacovazzo C.; Guagliardi, A. *J. Appl. Cryst.* **1993**, *26*, 343.
- 12 Sheldrick, G. M. SHELXL-97. Program for the refinement of crystal structures. University of Göttingen, Germany, 1997.
- 13 Spek, A. L. PLATON, A multipurpose crystallographic tool, Utrecht University, Utrecht, The Netherlands, 1999.
- 14 Farrugia, L. J. WinGX suite for small molecule single-crystal crystallography. *J. Appl. Cryst.* **1999**, *32*, 837.
- 15 SCALE3 ABSPACK - An Oxford Diffraction program (1.0.4,gui:1.0.3) (C), Oxford Diffraction Ltd., 2005.
- 16 (a) N. Fischer, T. M. Klapötke, D. G. Piercey, J. Stierstorfer, *Z. Anorg. Allg. Chem.* **2012**, *638*, 302–310; (b) N. Fischer, T. M. Klapötke, J. Stierstorfer, *Z. Anorg. Allg. Chem.* **2011**, *637*, 1273–1276.
- 17 T. M. Klapötke, J. Stierstorfer, A. Wallek, *Chem. Mater.* **2008**, *20*, 4519–4530.
- 18 (a) J. W. Ochterski, G. A. Petersson, and J. A. Montgomery Jr., A complete basis set model chemistry. V. Extensions to six or more heavy atoms, *J. Chem. Phys.* **1996**, *104*, 2598; (b) J. A. Montgomery Jr., M. J. Frisch, J. W. Ochterski G. A. Petersson, A

- complete basis set model chemistry. VII. Use of the minimum population localization method, *J. Chem. Phys.* **2000**, *112*, 6532.
- 19 (a) L. A. Curtiss, K. Raghavachari, P. C. Redfern, J. A. Pople, Assessment of Gaussian-2 and density functional theories for the computation of enthalpies of formation, *J. Chem. Phys.* **1997**, *106*, 1063; (d) E. F. C. Byrd, B. M. Rice, Improved Prediction of Heats of Formation of Energetic Materials Using Quantum Chemical Methods, *J. Phys. Chem. A* **2006**, *110*, 1005–1013; (d) B. M. Rice, S. V. Pai, J. Hare, Predicting Heats of Formation of Energetic Materials Using Quantum Chemical Calculations, *Comb. Flame* **1999**, *118*, 445–458.
- 20 P. J. Lindstrom, W. G. Mallard (Editors), NIST Standard Reference Database Number 69, <http://webbook.nist.gov/chemistry/> (Juni **2011**).
- 21 M. J. Frisch, G. W. Trucks, H. B. Schlegel, G. E. Scuseria, M. A. Robb, J. R. Cheeseman, G. Scalmani, V. Barone, B. Mennucci, G. A. Petersson, H. Nakatsuji, M. Caricato, X. Li, H.P. Hratchian, A. F. Izmaylov, J. Bloino, G. Zheng, J. L. Sonnenberg, M. Hada, M. Ehara, K. Toyota, R. Fukuda, J. Hasegawa, M. Ishida, T. Nakajima, Y. Honda, O. Kitao, H. Nakai, T. Vreven, J. A. Montgomery, Jr., J. E. Peralta, F. Ogliaro, M. Bearpark, J. J. Heyd, E. Brothers, K. N. Kudin, V. N. Staroverov, R. Kobayashi, J. Normand, K. Raghavachari, A. Rendell, J. C. Burant, S. S. Iyengar, J. Tomasi, M. Cossi, N. Rega, J. M. Millam, M. Klene, J. E. Knox, J. B. Cross, V. Bakken, C. Adamo, J. Jaramillo, R. Gomperts, R. E. Stratmann, O. Yazyev, A. J. Austin, R. Cammi, C. Pomelli, J. W. Ochterski, R. L. Martin, K. Morokuma, V. G. Zakrzewski, G. A. Voth, P. Salvador, J. J. Dannenberg, S. Dapprich, A. D. Daniels, O. Farkas, J.B. Foresman, J. V. Ortiz, J. Cioslowski, D. J. Fox, Gaussian 09 A.02, Gaussian, Inc., Wallingford, CT, USA, **2009**.
- 22 M. S. Westwell, M. S. Searle, D. J. Wales, D. H. Williams, Empirical correlations between thermodynamic properties and intermolecular forces, *J. Am. Chem. Soc.* **1995**, *117*, 5013-5015; (b) F. Trouton, On Molecular Latent Heat, *Philos. Mag.* **1884**, *18*, 54–57.
- 23 (a) H. D. B. Jenkins, H. K. Roobottom, J. Passmore, L. Glasser, Relationships among Ionic Lattice Energies, Molecular (Formula Unit) Volumes, and Thermochemical Radii, *Inorg. Chem.* **1999**, *38*, 3609-3620. (b) H. D. B. Jenkins, D. Tudela, L. Glasser, Lattice Potential Energy Estimation for Complex Ionic Salts from Density Measurements, *Inorg. Chem.* **2002**, *41*, 2364–2367.
- 24 M. Göbel, K. Karaghiosoff, T. M. Klapötke, D. G. Piercey, Nitrotetrazolate, *J. Am. Chem. Soc.* **2010**, *132*, 17216–17226.

- 25 D. E. Wilcox, L. A. Bromley, *J. Chem. Eng.* **1963**, *55*, 32–39.
- 26 V. Rafeev, Y. Rubtsov, *Russ. Chem. Bull.* **1993**, *42*, 1811–1815.
- 27 T. M. Klapötke, A. Preimesser, J. Stierstorfer, *Z. Anorg. Allg. Chem.* **2012**, *638*, 1278–1286.
- 28 N. Fischer, T. Klapötke, M. Reymann, J. Stierstorfer, *Eur. J. Inorg. Chem.* **2013**, *2013*, 2167–2180.
- 29 D. Fischer, T. Klapötke, J. Stierstorfer, *Angew. Chem.* **2014**, *126*, 8311–8314.
- 30 M. Zimmer, E. Baroody, G. Carpenter, R. Robb, *J. Chem. Eng. Data* **1968**, *13*, 212–214.
- 31 J. E Felts, H. W. Sandusky, R. H. Granholm, *AIP Conf. Proc.* **2009**, *1195*, 233.
- 32 H. W. Sandusky, R. H. Granholm, D. G. Bohl, IHTR 2701, Naval Surface Warfare Center, Indian Head, MD, 12 Aug 2005.
- 33 R. Mayer, J. Köhler, A. Homburg, *Explosives*, 5th ed., Wiley VCH, Weinheim, **2002**, 197–200.
- 34 R. Mayer, J. Köhler, A. Homburg, *Explosives*, 5th ed., Wiley VCH, Weinheim, **2002**, 148.
- 35 T. M. Klapötke, P. Mayer, C. M. Sabaté, J. M. Welch, N. Wiegand, *Inorg. Chem.* **2008**, *47*, 6014–6027.
- 36 S. Kim, J. Kim, *Bull. Korean Chem. Soc.* **2013**, *34*, 2503–2506.
- 37 M. I. Saleh, E. Kusrini, R. Adnan, B. Saad, B. M. Yamin, H. K. Fun, , *J. Mol. Struct.* **2007**, *837*, 169–178.
- 38 F. A. Miller, C. H. Wilkins, *Anal. Chem.* **1952**, *42*, 1253–1294.
- 39 M. Hesse, H. Meier and B. Zeeh, *Spektroskopische Methoden in der Organischen Chemie*, Thieme, Stuttgart, New York, 7th edn, 2005.